

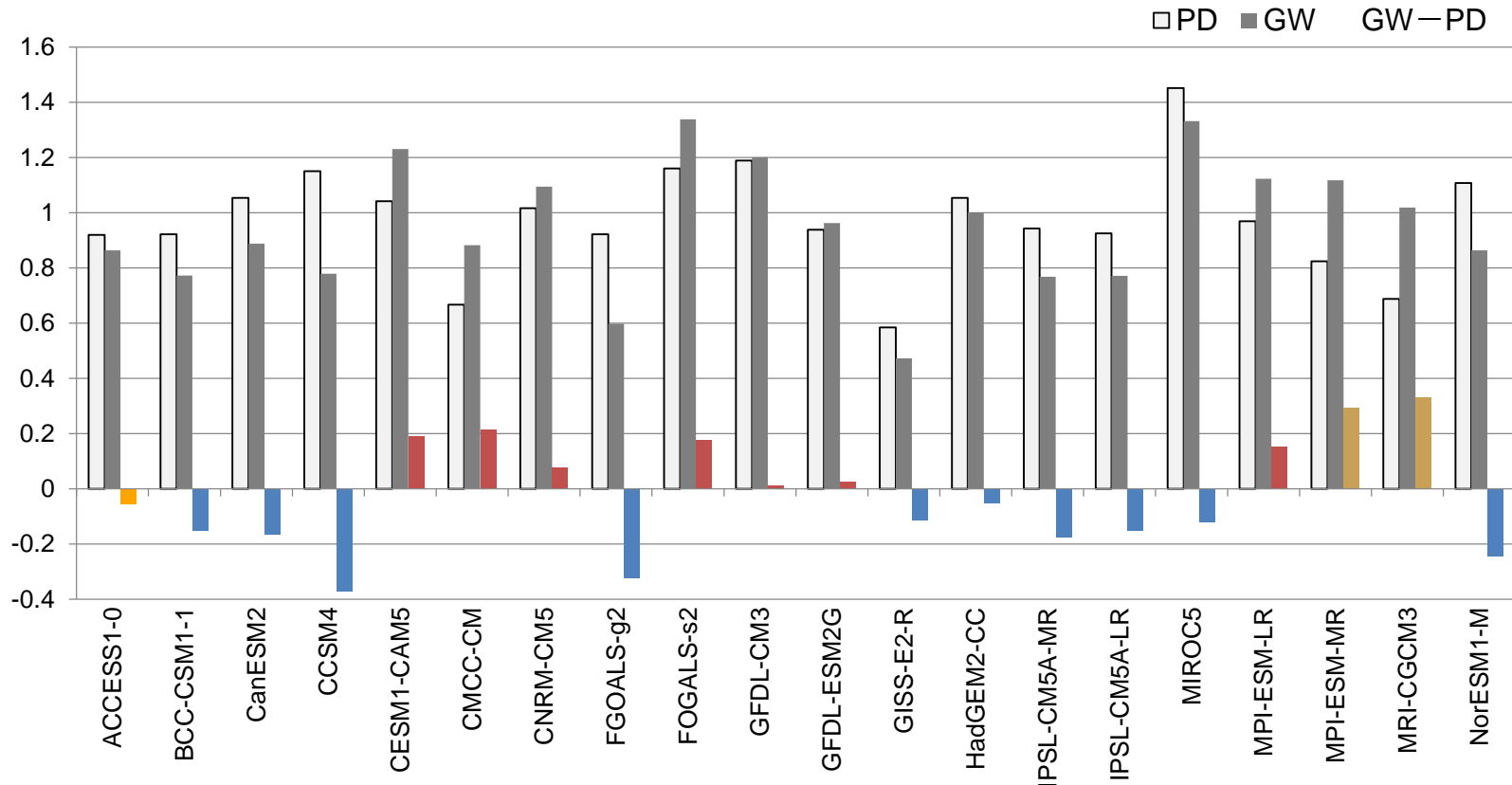
Diagnosis of ENSO/IOD Positive and Negative Air-Sea Feedback Strength in Coupled GCMs

Tim Li

**Department of Atmospheric Sciences and IPRC
University of Hawaii**

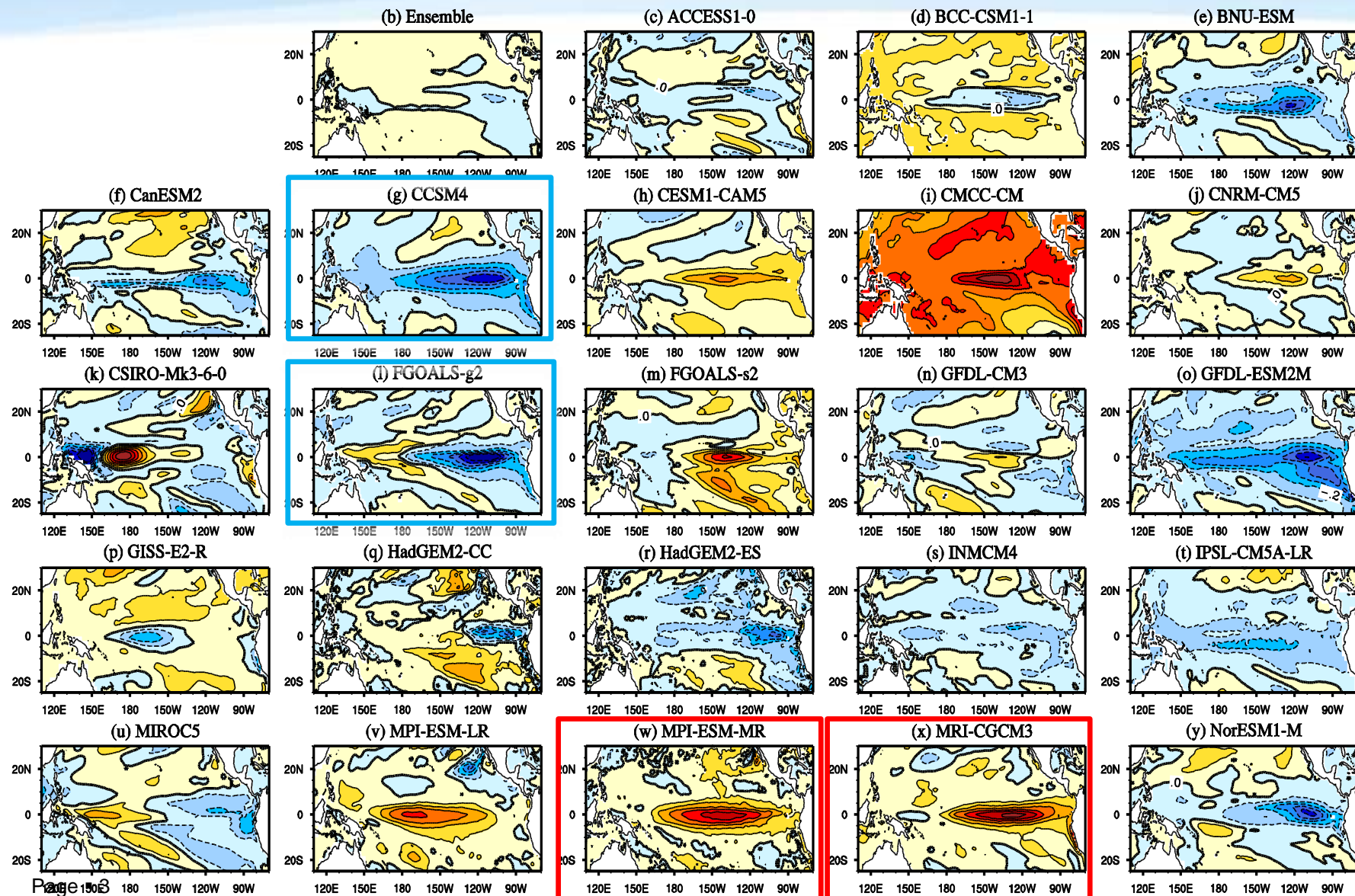
Nino3 SSTA Standard Deviation in CMIP5 models

PD = Present Day Climate State
GW = Global Warming Climate State

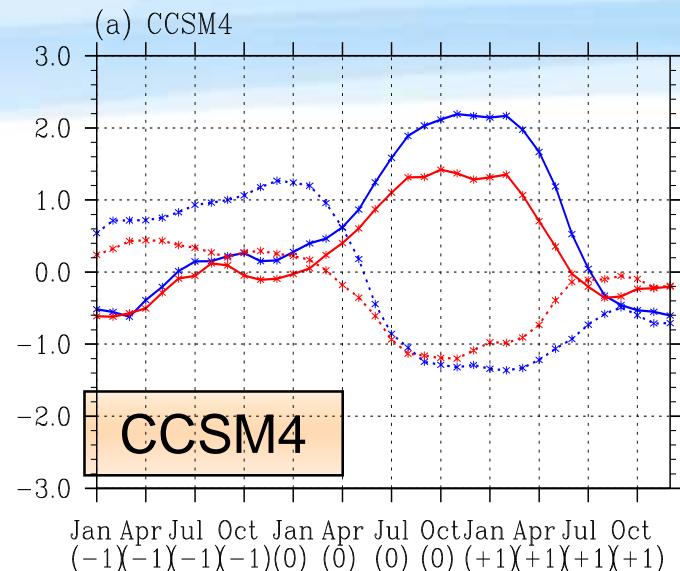


Change of SSTA STD pattern: RCP85 (2051-2100) minus historical (1951-2000)

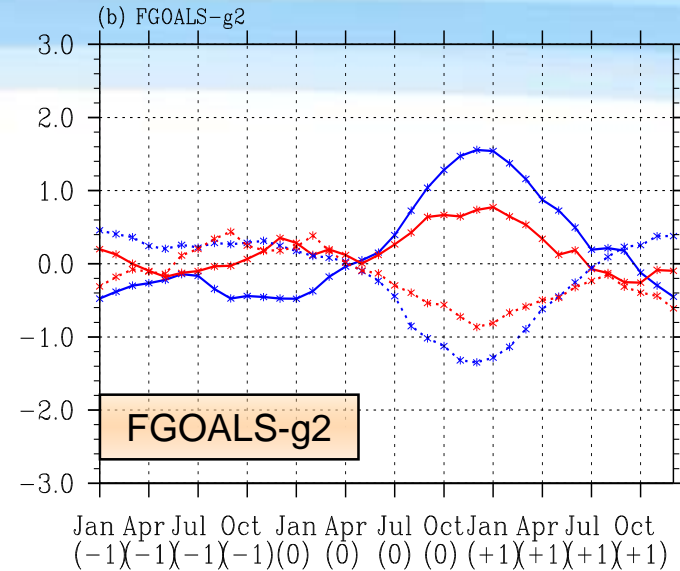
(SST has been de-trended)



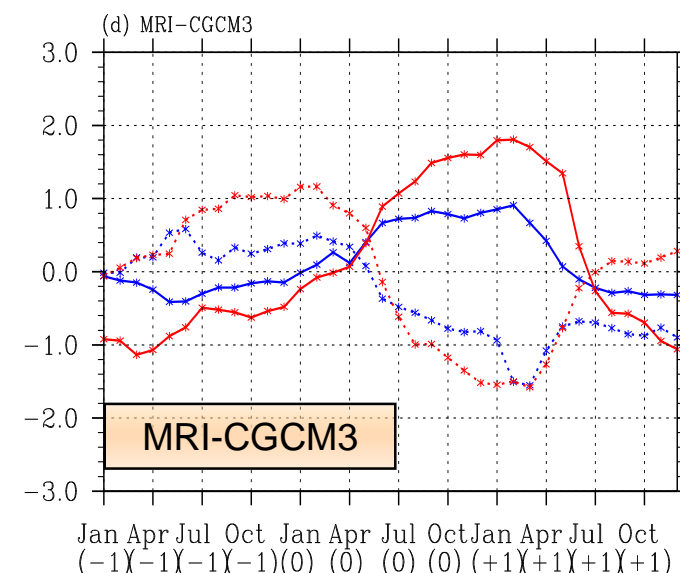
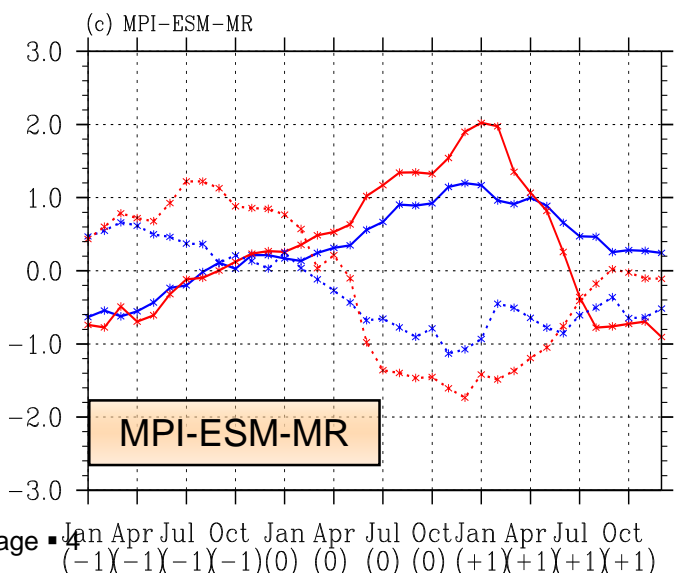
Composite evolutions of El Niño and La Niña in 4 CGCMs



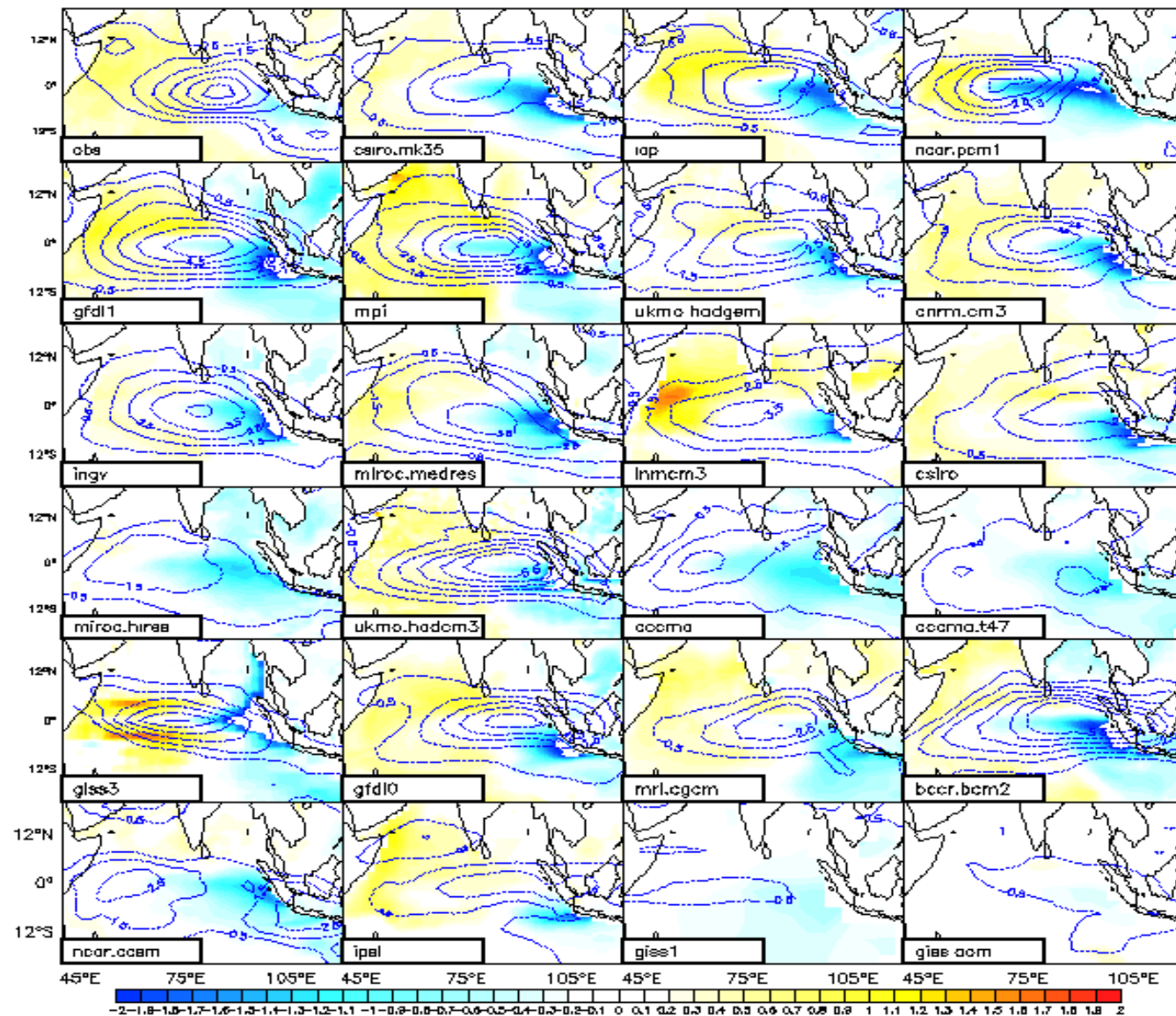
PD
GW



PD
GW

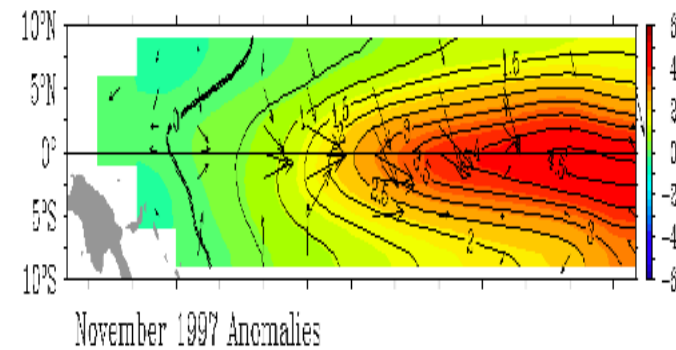
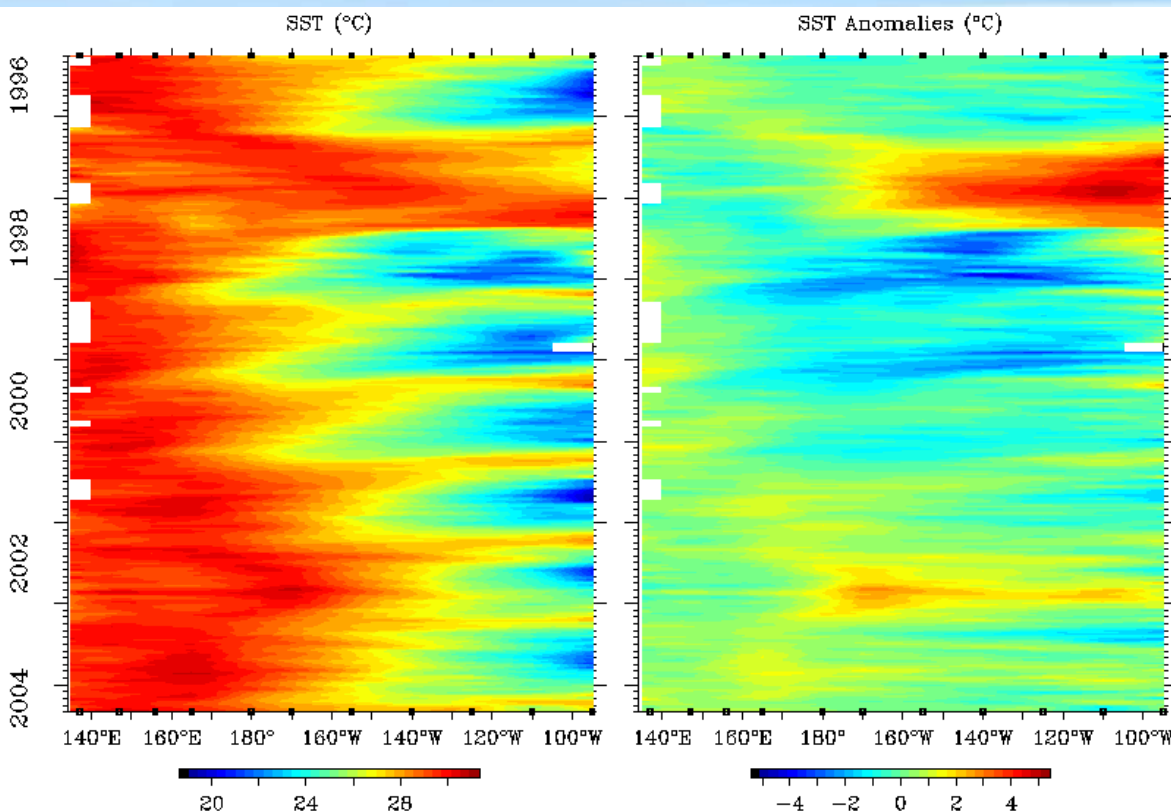


Composite SSTA (shading) and 850-hPa zonal wind anomaly fields in SON from the observation and 23 CMIP3 models



For given a coupled model, the ENSO strength might be weaker (or stronger) than the observed. How do you know which part of model air-sea feedback processes (atmospheric response to SST, ocean response to the wind, cloud radiative forcing, and/or surface latent heat flux) are incorrect?

1. Introduction: What is El Nino?

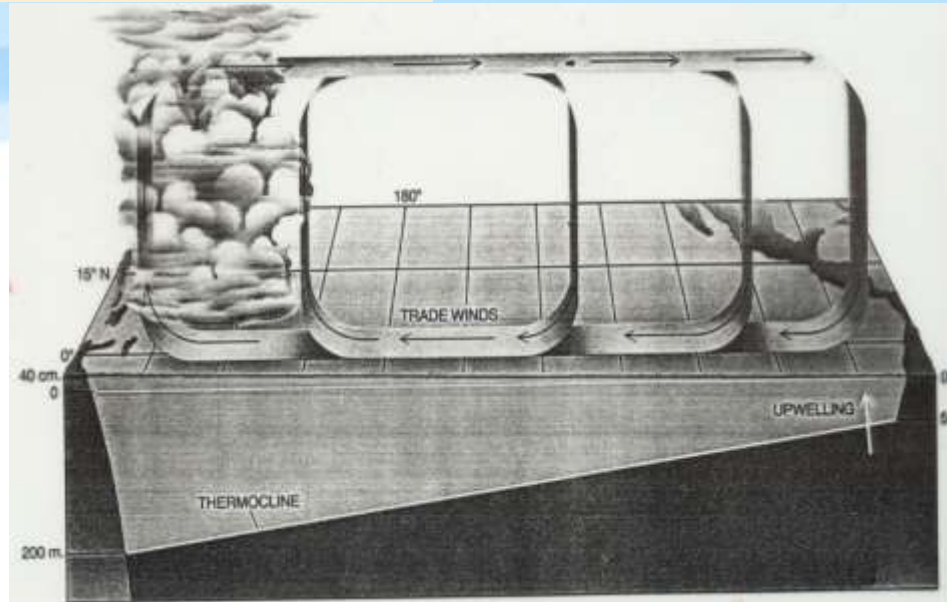


Fundamental science question related to El Nino:

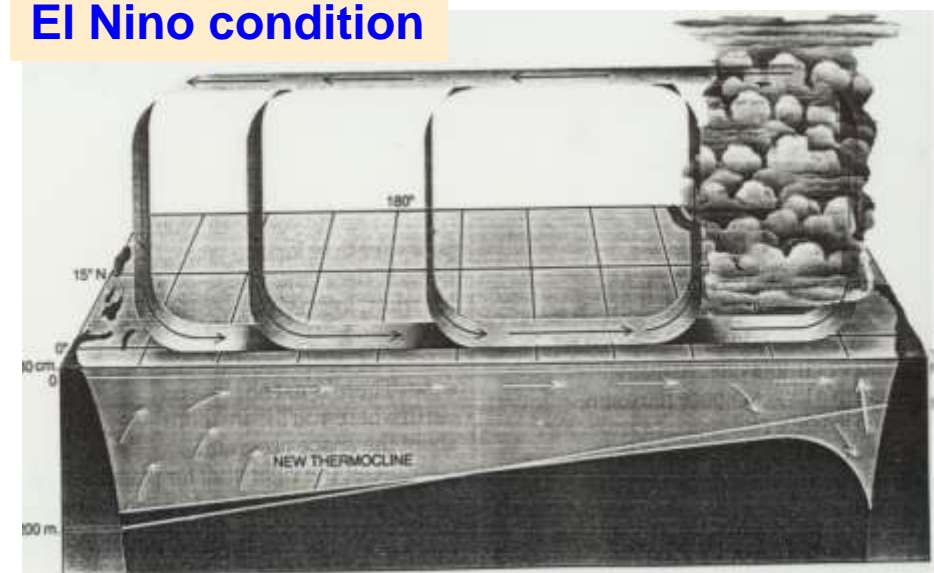
- What causes the growth of El Nino?

Atmosphere-ocean interactions (Bjerknes 1969, Philander et al. 1984, Hirst 1986, 1988, ...)

Normal condition



El Nino condition



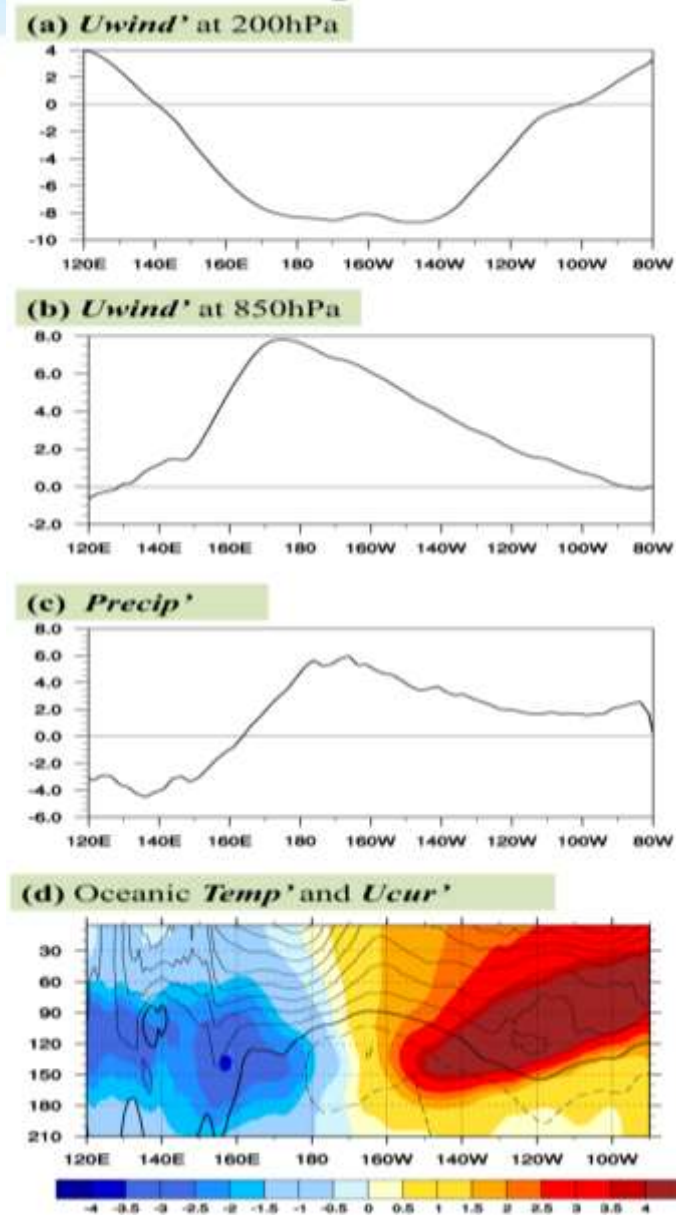
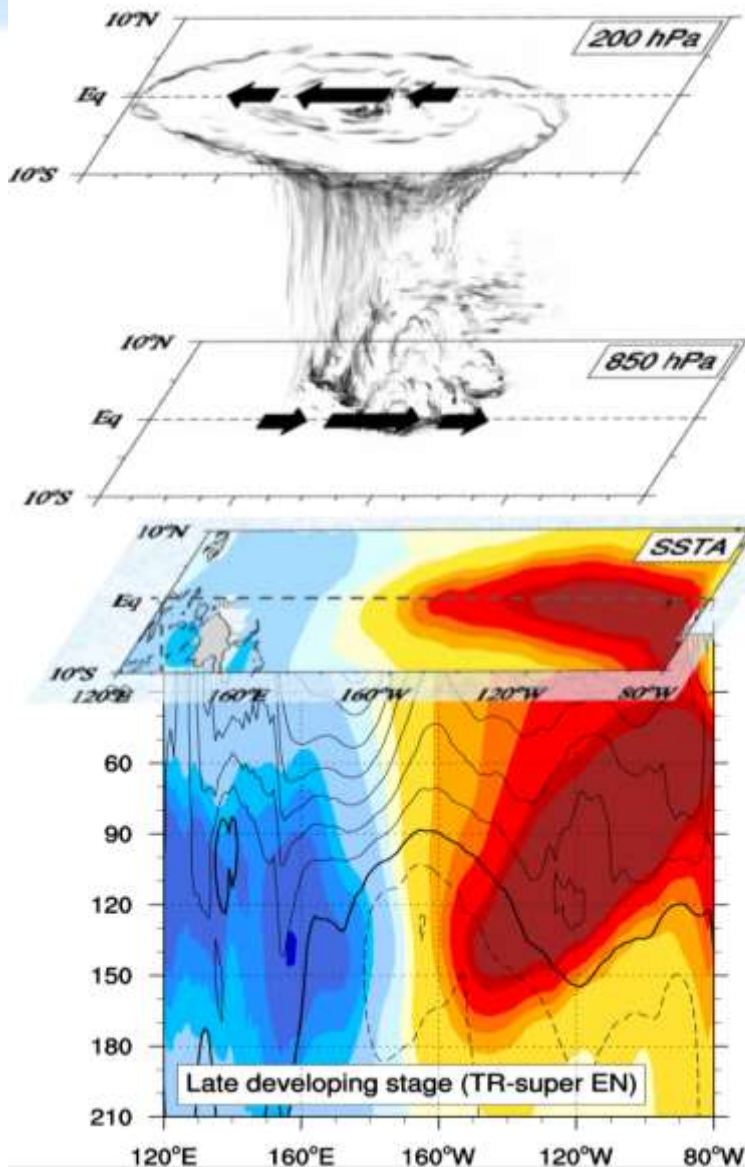
J. Bjerknes (1969) first termed the equatorial atmospheric zonal overturning circulation as “Walker circulation”.

Three positive feedbacks:

- Zonal advective feedback
- Ekman feedback
- Thermocline feedback

$$\frac{\partial T}{\partial t} \approx -u \bar{T}_x - w \bar{T}_z - \bar{w} T_z$$

3-Dimensional Structure of El Niño

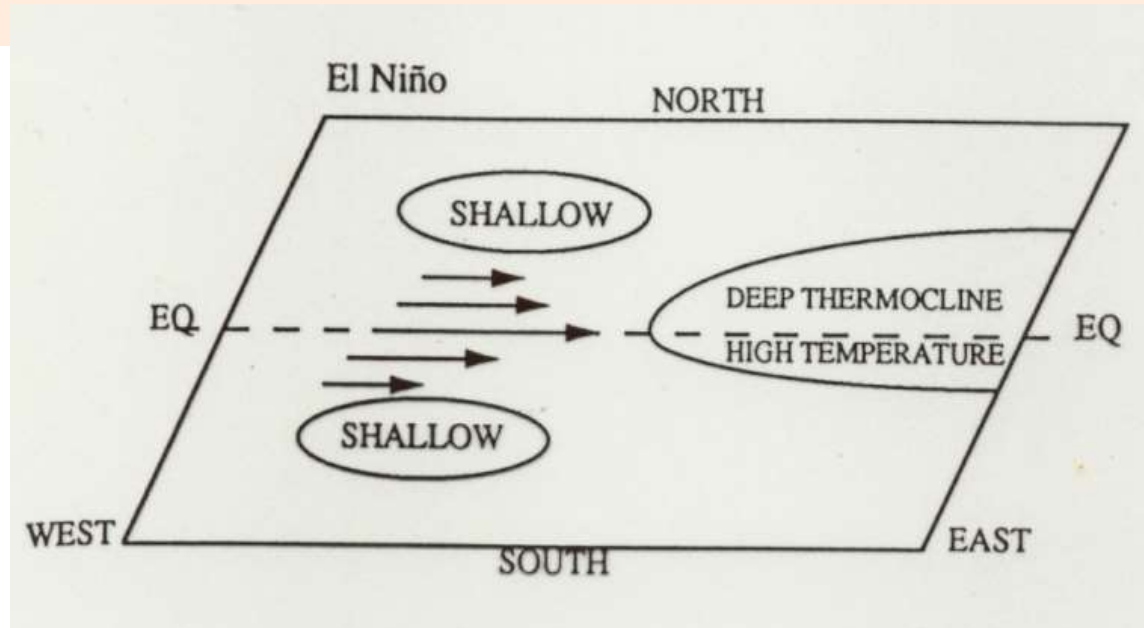


1. Introduction (cont.)

Another science question related to El Niño dynamics:

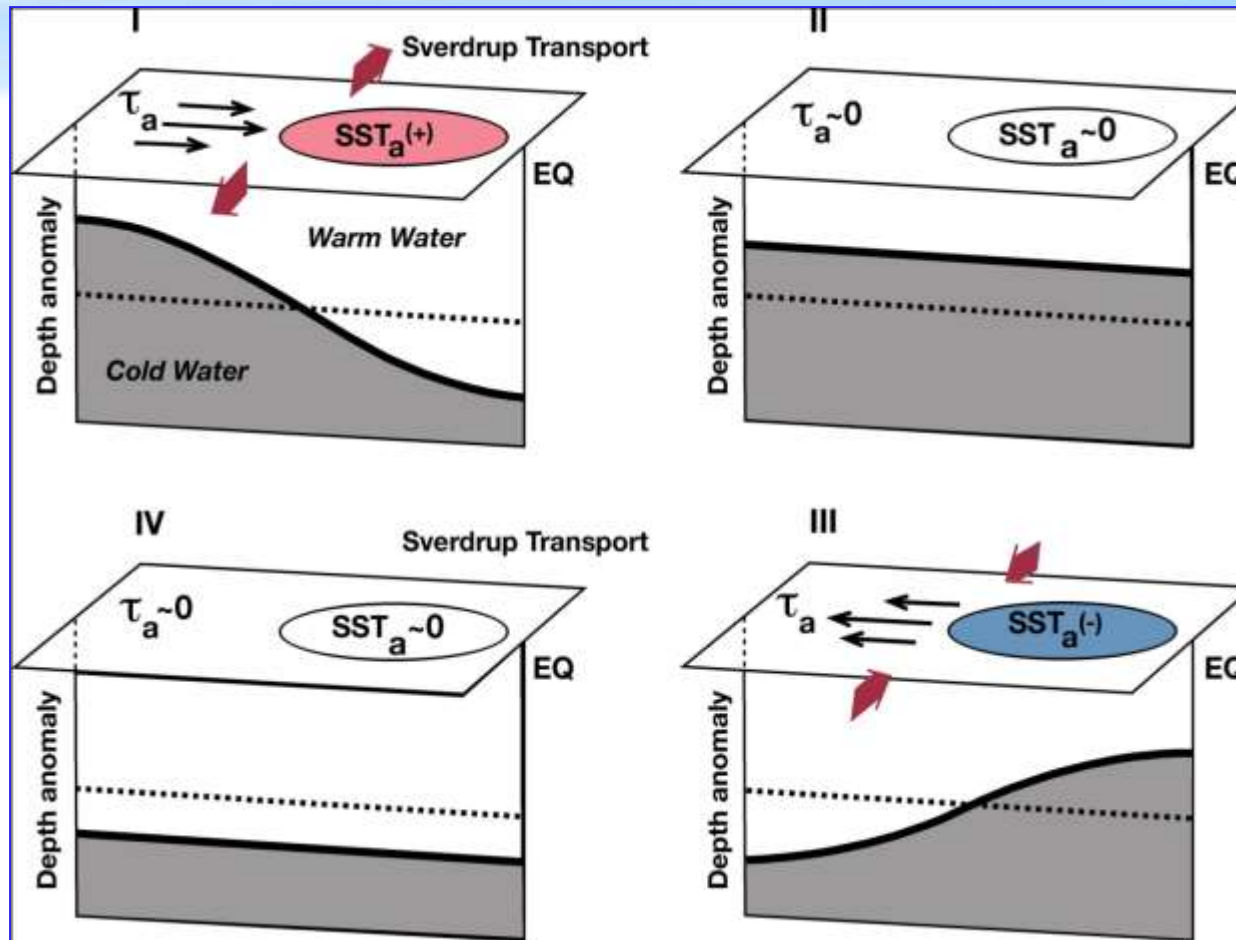
➤ What causes the oscillation?

1. Delayed Oscillator mode (McCreary and Anderson 1983, Schopf and Sureaz 1988, Battisiti and Hirst 1989, ...)



Key: delayed negative effect of ocean waves

2. Recharge Oscillator Theory (Jin 1997, Li 1997)



$$\frac{dT}{dt} = /T + wh$$
$$\frac{dh}{dt} = -WT,$$

T: EEP SSTA

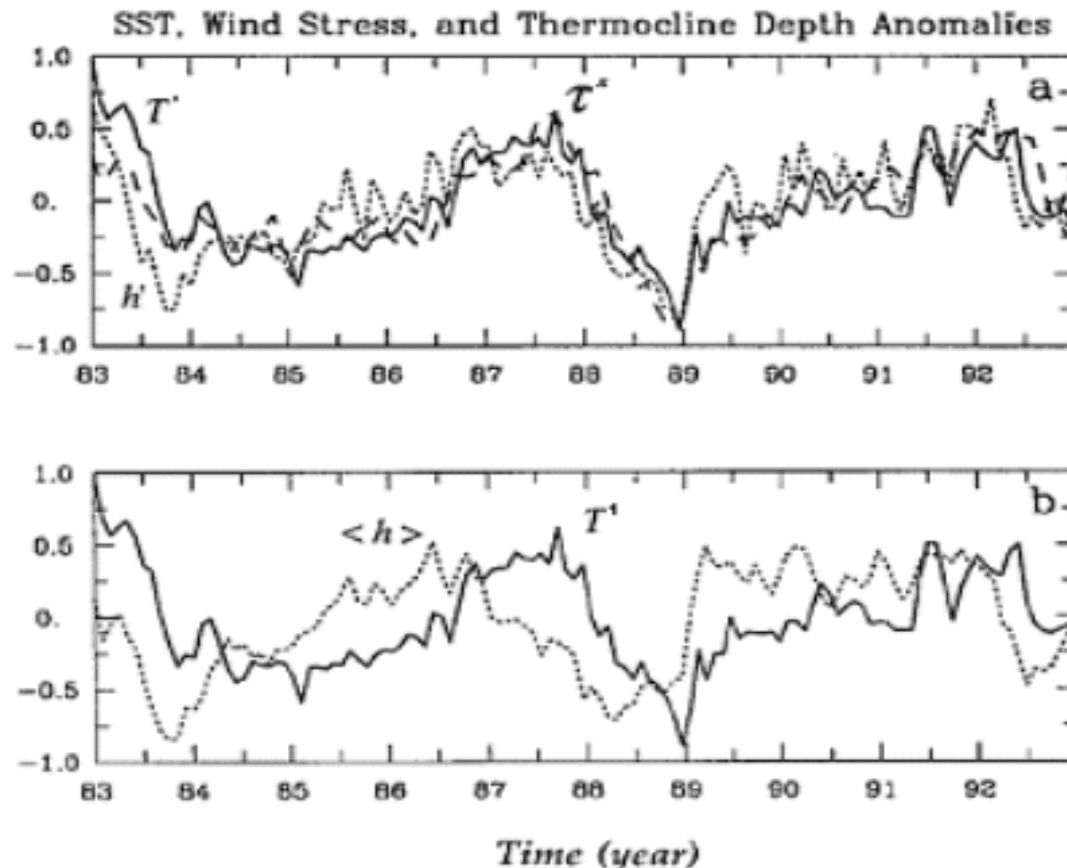
h: WEP thermocline depth anomaly

Meinen & McPhaden, 2000

Key: Wind stress curl induced Sverdrup transport leads to zonal mean thermocline depth change at the equator

NMC ocean assimilation data revealed the observed SSTA – zonal mean thermocline anomaly $\langle h \rangle$ relationship (Li 1997)

h' , T' , τ^*
in phase



$$\frac{\partial \langle h \rangle}{\partial t} \propto -T'$$

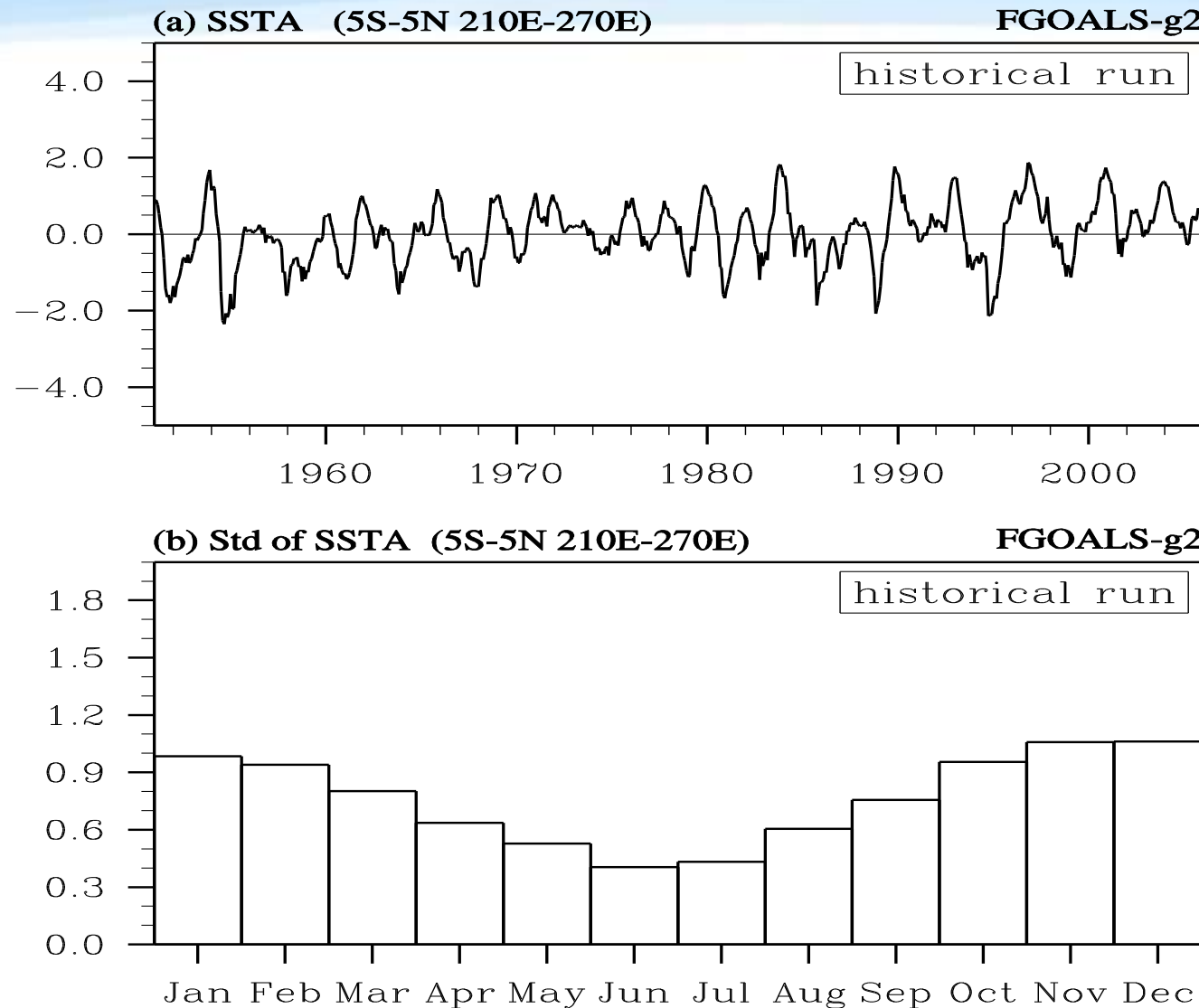
T' SST anomaly in the eastern equatorial Pacific

τ^* Zonal wind stress in the central equatorial Pacific

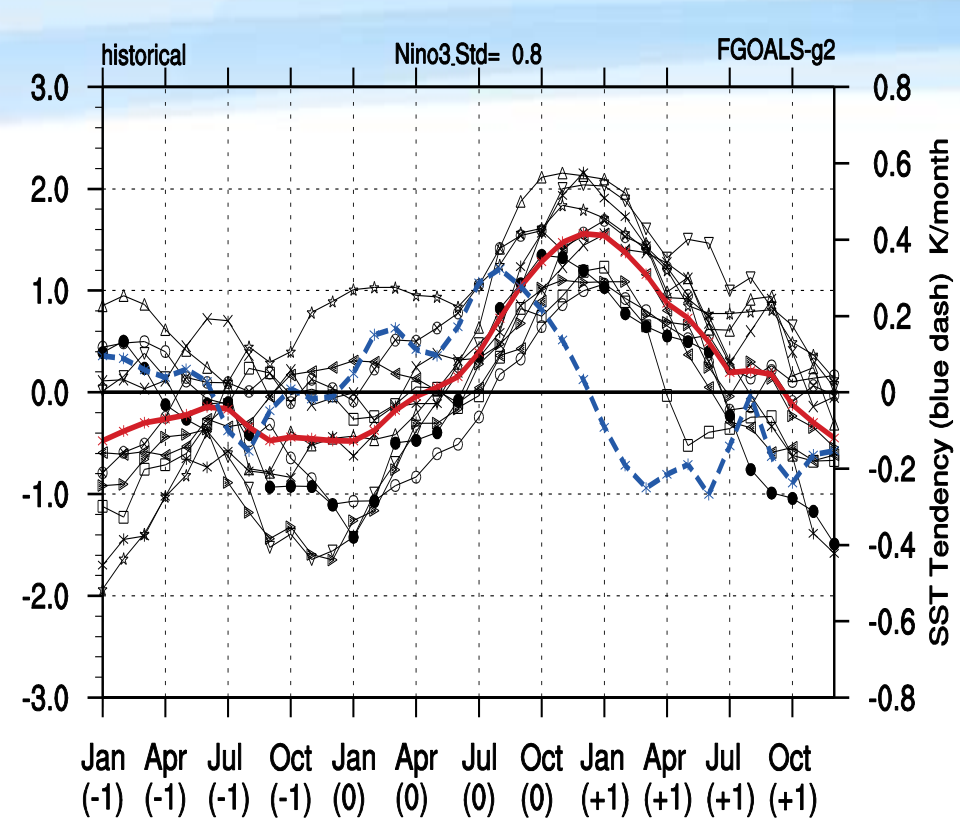
$h' = h_e - h_w$ h' Zonally asymmetric thermocline depth anomaly

$\langle h \rangle$ Zonal mean thermocline depth anomaly

Example 1: Time series of Niño3 SSTA in FGOALS-G2



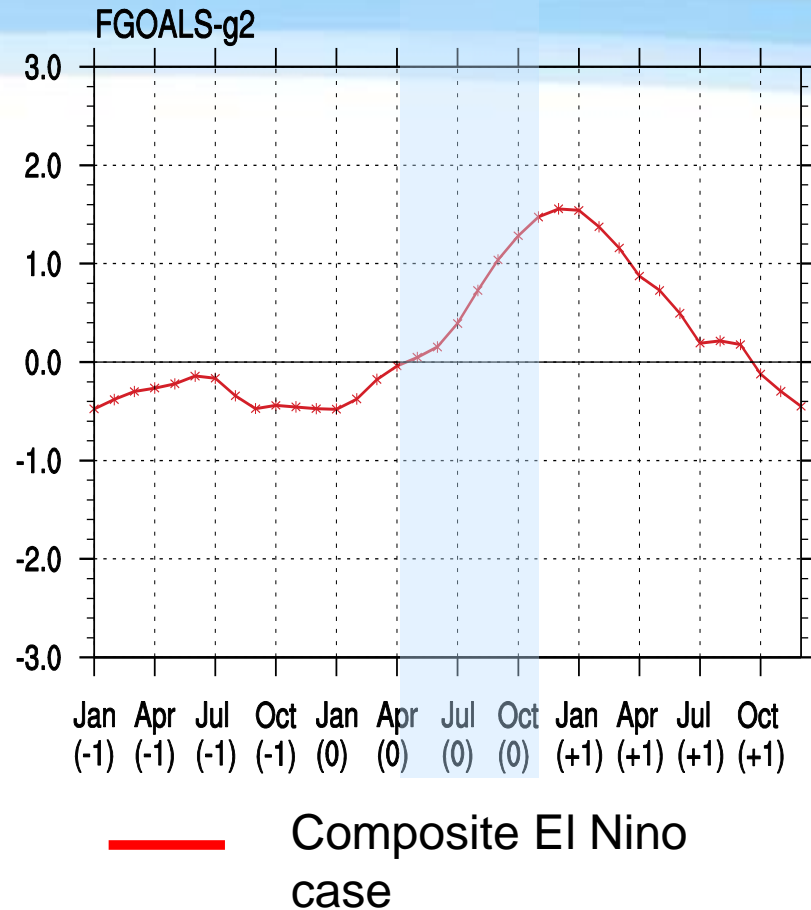
Composite Time Series of SSTA in Nino3



— EI Nino cases

— Composite El Nino case

— SST-tendency of the composite El Nino case



— Composite El Nino case

Diagnose the SSTA-tendency during **developing phase (Apr-Nov[0])** for composite El Nino

Mixed-layer temperature tendency equation

ML temperature tendency equation:

$$\begin{aligned}\partial T'/\partial t = & -u' \partial \bar{T}/\partial x - \bar{u} \partial T'/\partial x - u' \partial T'/\partial x - w' \partial \bar{T}/\partial z - \bar{w} \partial T'/\partial z - w' \partial T'/\partial z \\ & \text{term 1} \quad \text{term 2} \quad \text{term 3} \quad \text{term 4} \quad \text{term 5} \quad \text{term 6} \\ & -v' \partial \bar{T}/\partial y - \bar{v} \partial T'/\partial y - v' \partial T'/\partial y + \frac{Q'_{net}}{\rho C_p H} + R \\ & \text{term 7} \quad \text{term 8} \quad \text{term 9} \quad \text{term 10}\end{aligned}$$

term 1 – term 10 are shown in the above equation

term 11: the sum of term1 to term 10;

term 12: the actual mixed layer temperature tendency

Bar: climatological seasonal cycle;

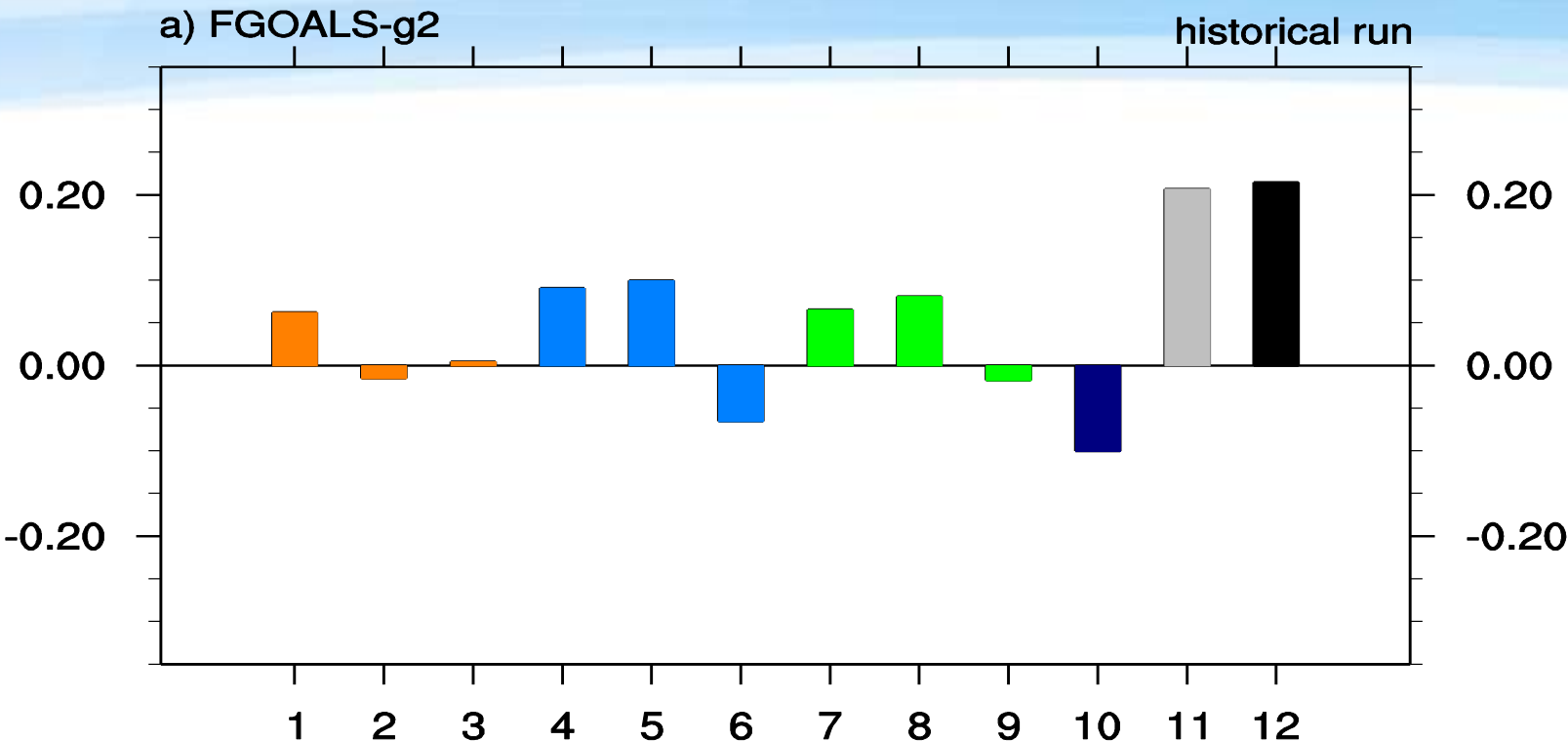
Prime: anomaly field with respect to the climatological seasonal cycle;

H: spatially and temporally varying mixed layer depth

R: residual term

$$Q_{net} = Q_{sw} - Q_{LW} - Q_{LH} - Q_{SH}$$

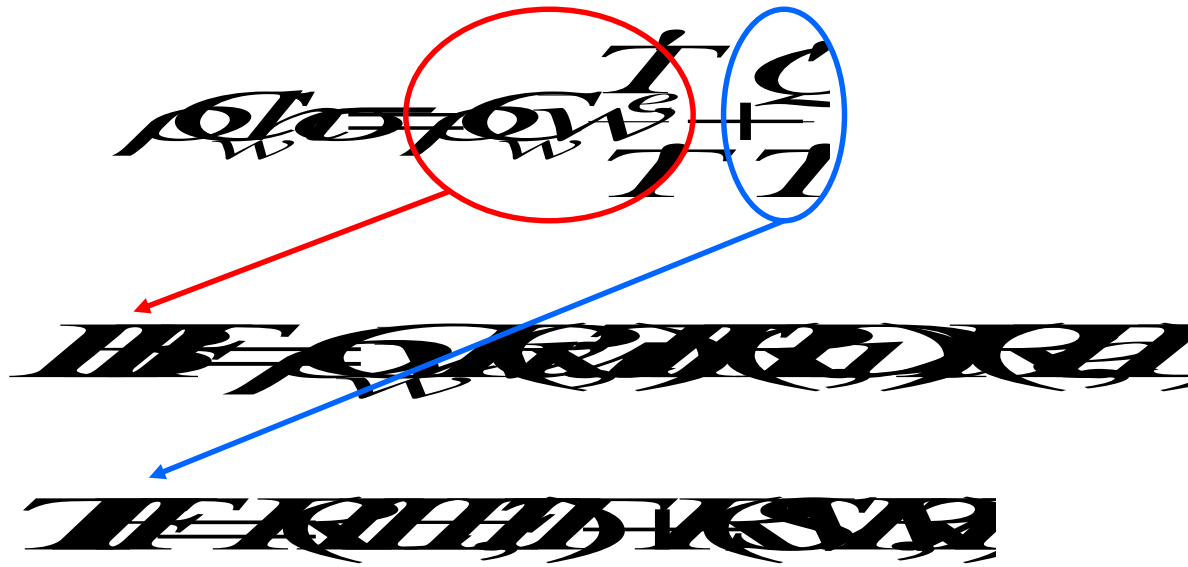
Mixed-Layer Heat Budget Diagnosis



The major contributing terms are zonal advective feedback (term 1), Ekman feedback (term4), thermocline feedback (term 5) and meridional advective feedback (term8)

$$\frac{d}{dt} = \frac{T}{h} + \frac{Q}{\rho L}$$

$$T = \delta T e^{\sigma t}$$



Combined dynamic and thermodynamic feedback index (CFI) may be written as:

$$CFI = BFI + TFI$$

Bjerkner's Thermocline feedback

Following previous studies (Liu, Li, et al. 2012; Chen, Li, et al. 2015), the growth rate associated with thermocline feedback can be written as:

$$\sigma = \frac{\bar{w}}{H} R(\tau'_x, T') R(D', \tau'_x) R(T'_e, D')$$

\bar{w} : mean vertical velocity; H : mixed layer depth

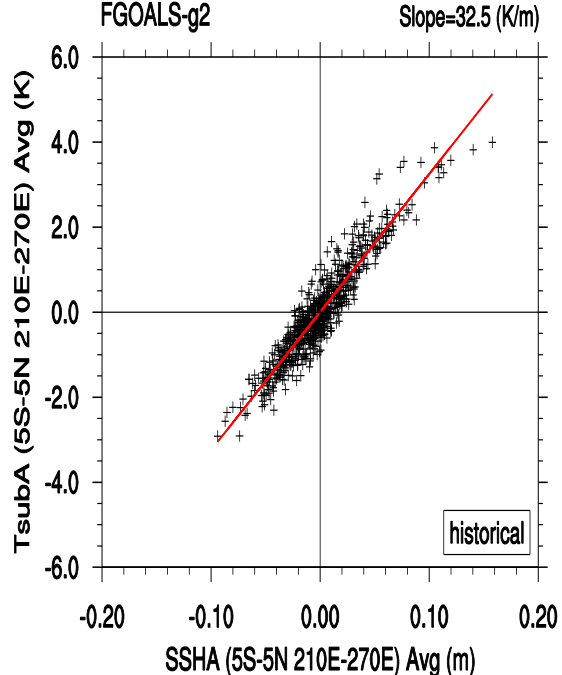
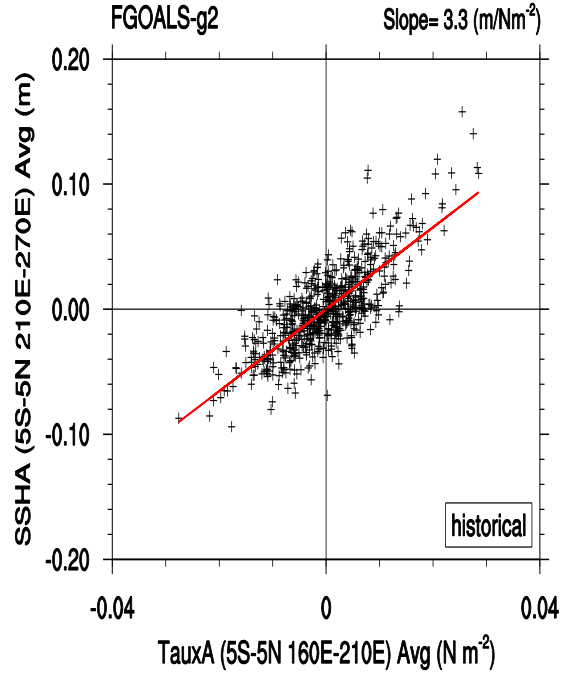
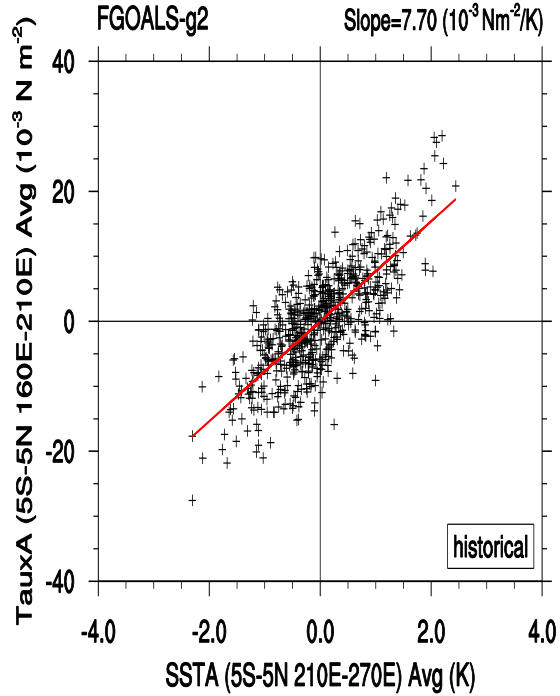
D' : thermocline depth anomaly; T'_e : subsurface ocean temperature anomaly

$R(\tau'_x, T')$: the atmospheric response of zonal wind stress anomaly (τ'_x) in the central equatorial Pacific (CEP) to a unit SSTA forcing in the eastern equatorial Pacific (EEP);

$R(D', \tau'_x)$: the response of ocean thermocline in EEP to a unit zonal wind stress (τ'_x) forcing in CEP;

$R(T'_e, D')$: the response of the ocean subsurface temperature to a unit thermocline depth change in EEP.

Three feedback processes

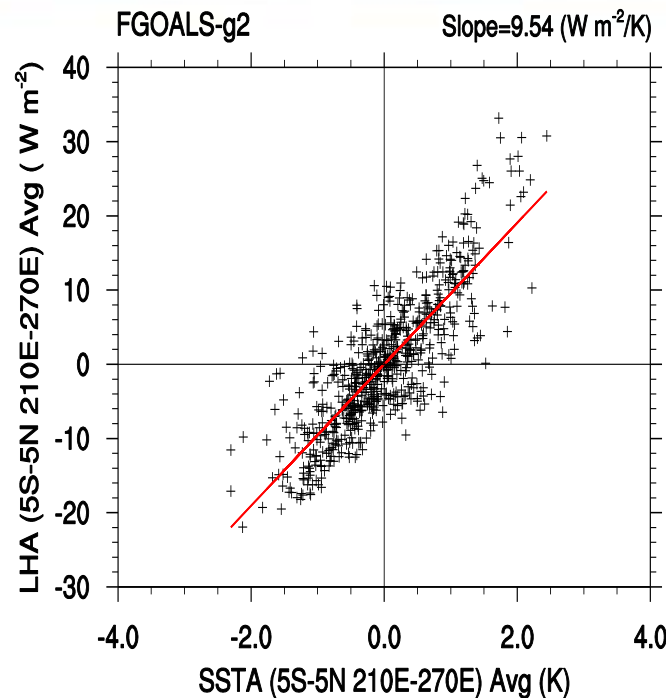
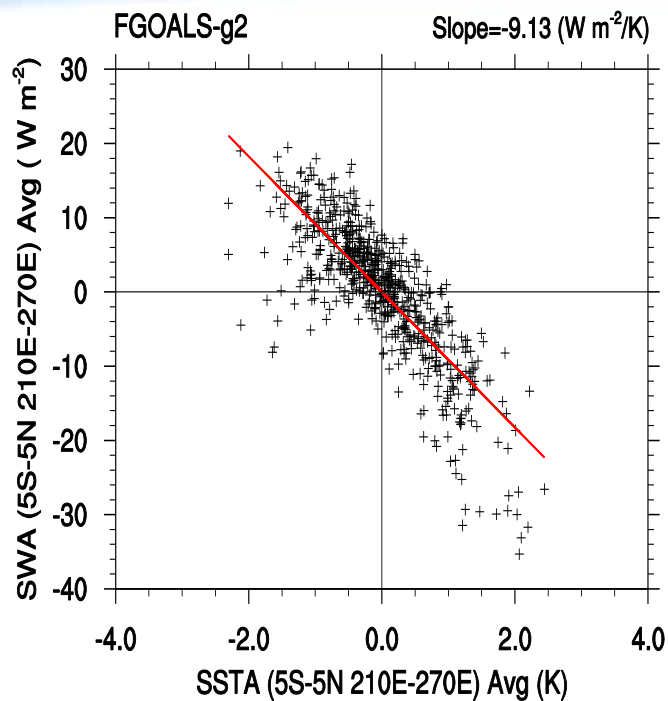


$$R(\tau_x', T')$$

$$R(D', \tau_x')$$

$$R(T_e', D')$$

Thermodynamic-related feedbacks (SW feedback and LH feedback)

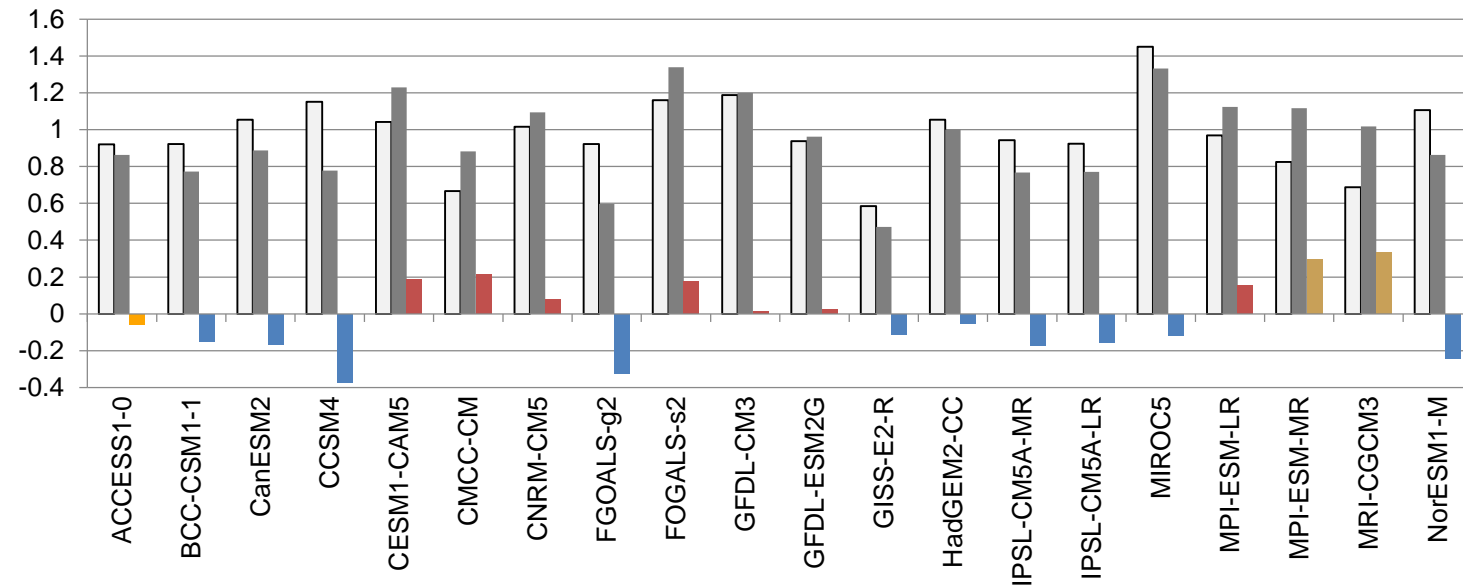


$$R(SW', T')$$

$$R(LH', T')$$

Example 2: Understand the cause of divergent projections of ENSO amplitude change under Global Warming in CMIP5 models

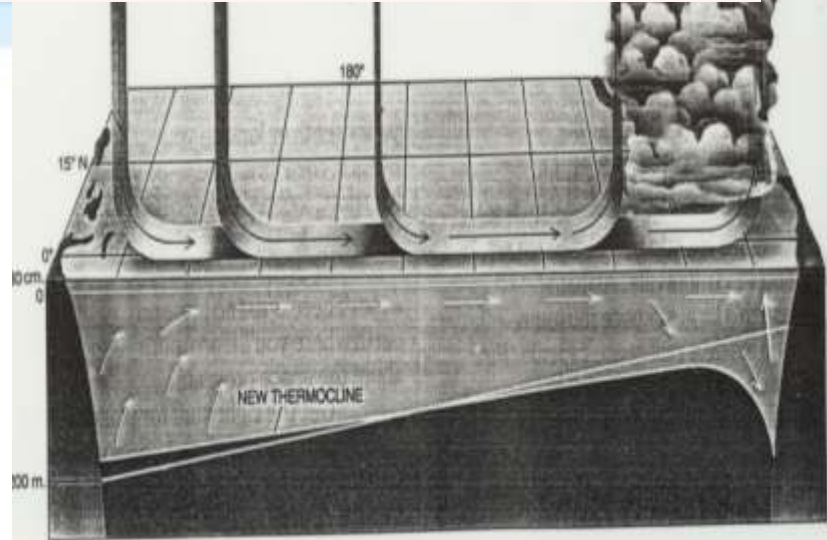
Nino3 SSTA Standard Deviation in PD, GW, GW-PD / GW-PD



ENSO development involves various positive feedbacks

$$\frac{\partial T}{\partial t} \approx -u \bar{T}_x - w \bar{T}_z - \bar{w} T_z$$

ZA Ekman TH

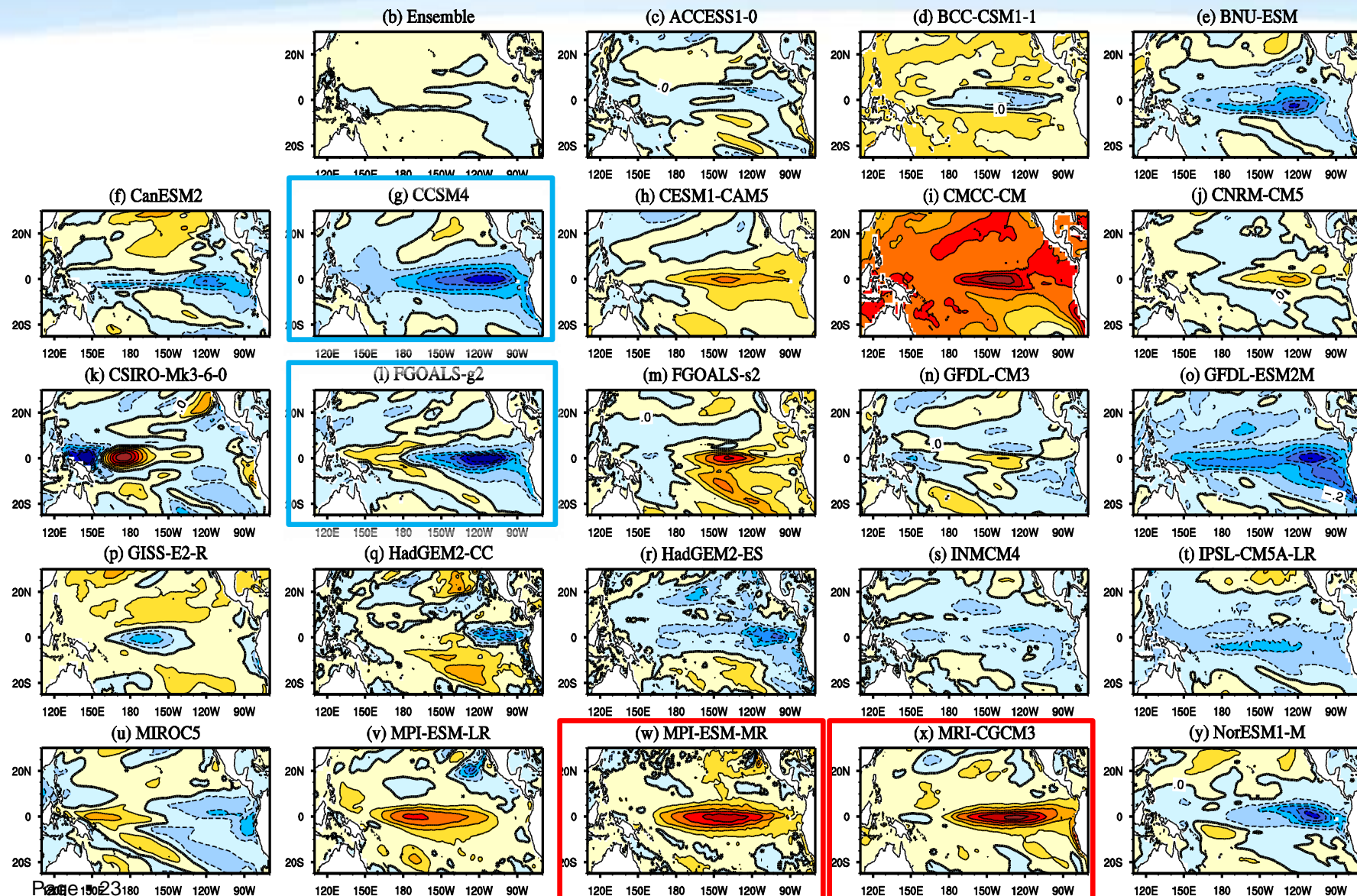


Science Question 1:

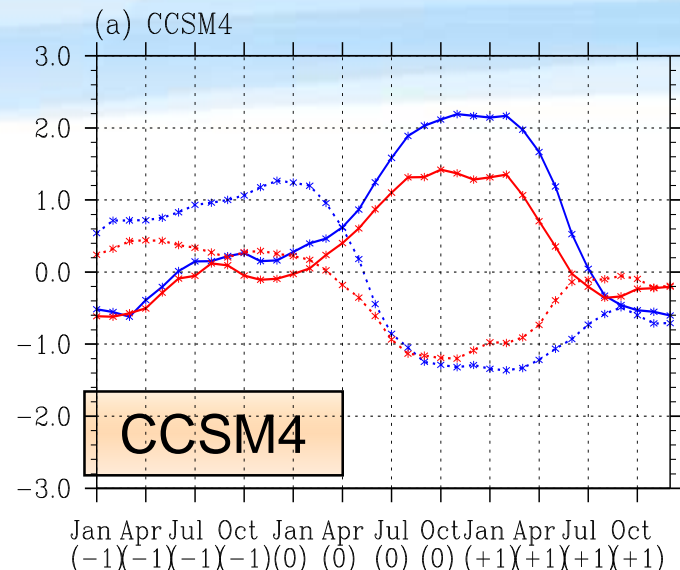
Which of the above positive feedback terms are main cause of divergent ENSO amplitude change projection under GW?

Change of SSTA STD pattern: RCP85 (2051-2100) minus historical (1951-2000)

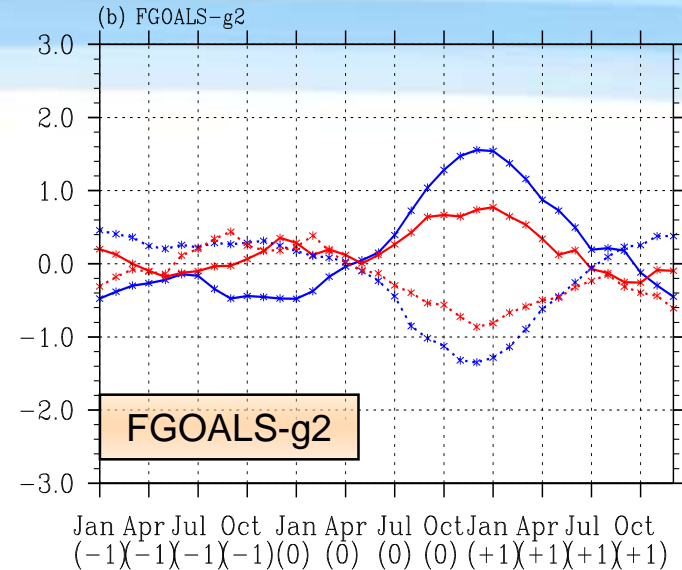
(SST has been de-trended)



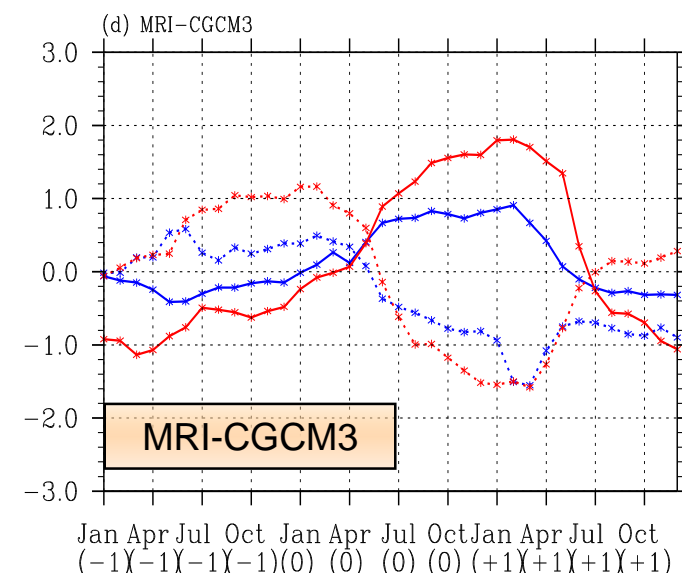
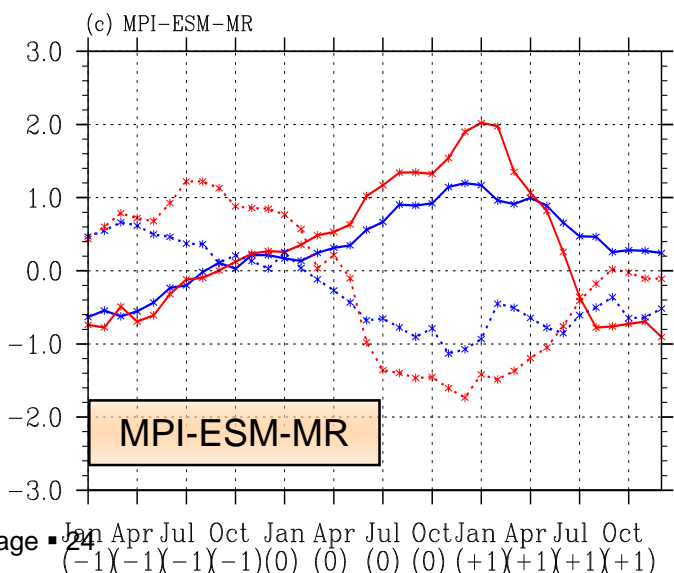
Composite evolutions of El Niño and La Niña in 4 CGCMs



PD
GW



PD
GW



Mixed-layer Heat Budget Analysis

The mixed layer temperature tendency equation:

$$\frac{\partial T'}{\partial t} = -u' \frac{\partial \bar{T}}{\partial x} - \bar{u}' \frac{\partial T'}{\partial x} - u' \frac{\partial T'}{\partial x} - w' \frac{\partial \bar{T}}{\partial z} - \bar{w}' \frac{\partial T'}{\partial z} - w' \frac{\partial T'}{\partial z}$$

(1) (2) (3) (4) (5) (6)

$$-v' \frac{\partial \bar{T}}{\partial y} - \bar{v}' \frac{\partial T'}{\partial y} - v' \frac{\partial T'}{\partial y} + \frac{Q'}{\rho C_p H} + R$$

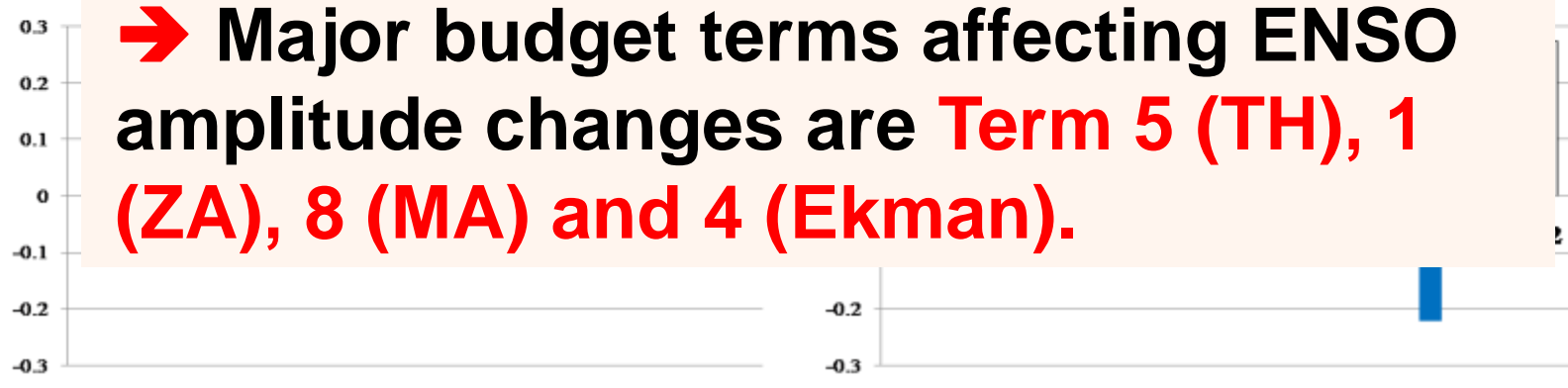
(7) (8) (9) (10)

We examine the MLT tendency during **ENSO developing phase** (Apr-Nov[year 0]) for each of the CGCMs.

Composite MLT Budget Terms (GW minus PD)



→ Major budget terms affecting ENSO amplitude changes are **Term 5 (TH)**, **1 (ZA)**, **8 (MA)** and **4 (Ekman)**.

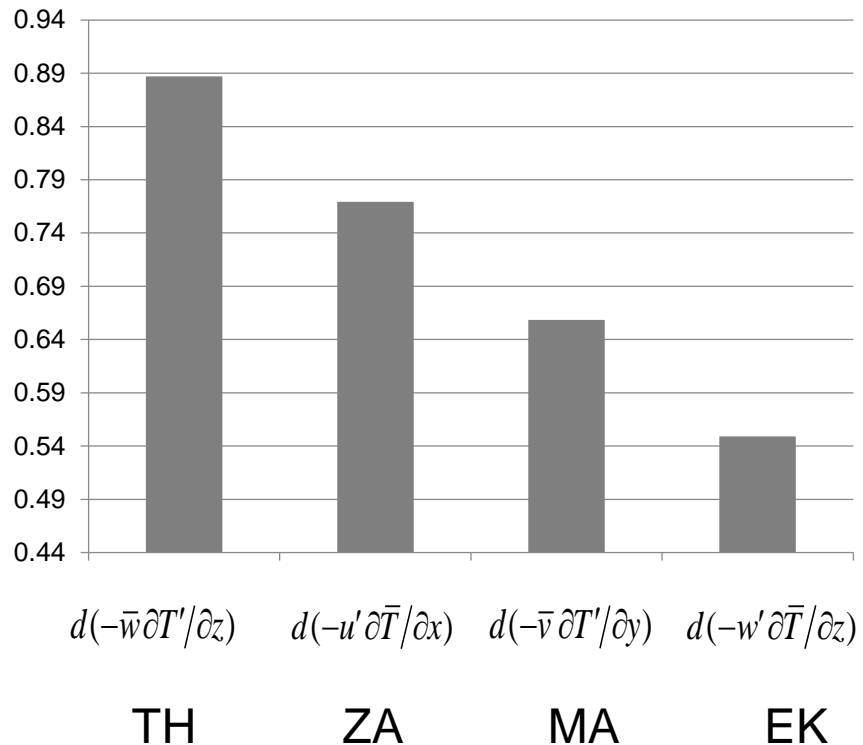


Term 1	Term 2	Term 3	Term 4	Term 5	Term 6	Term 7	Term 8	Term 9	Term 10	Term 11	Term 12
--------	--------	--------	--------	--------	--------	--------	--------	--------	---------	---------	---------

0.41	0.01	-0.10	0.22	0.54	0.01	0.01	0.32	-0.06	-0.5	0.86	0.88
------	------	-------	------	------	------	------	------	-------	------	------	------

- (1) $d(-u' \partial \bar{T} / \partial x)$ (2) $d(-\bar{u} \partial T' / \partial x)$ (3) $d(-u' \partial T' / \partial x)$ (4) $d(-w' \partial \bar{T} / \partial z)$ (5) $d(-\bar{w} \partial T' / \partial z)$ (6) $d(-w' \partial T' / \partial z)$
 Page ■ 26
 (7) $d(-v' \partial \bar{T} / \partial y)$ (8) $d(-\bar{v} \partial T' / \partial y)$ (9) $d(-v' \partial T' / \partial y)$ (10) $d(Q' / \rho C_p H)$ (11) $d(\text{Adv+Qnet})$ (12) $d(\partial T' / \partial t)$

Correlation between ENSO Amplitude Change and MLT Budget Terms among 20 CMIP5 models



95% confidence level: 0.44

→ **TH and ZA feedbacks** are major drivers for the divergent ENSO amplitude changes.

Science Question 2:

The changes of all feedbacks mentioned above involve both the changes of the **mean state** and **perturbation**. Which change, **mean state or perturbation change**, is critical in determining the MLT tendency change?

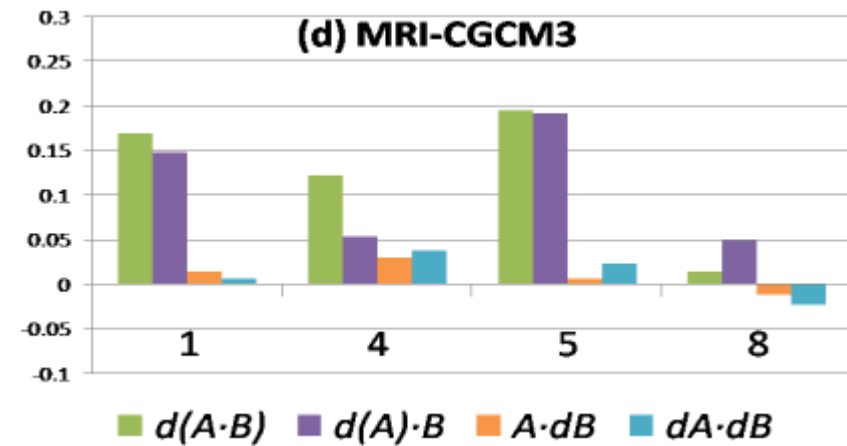
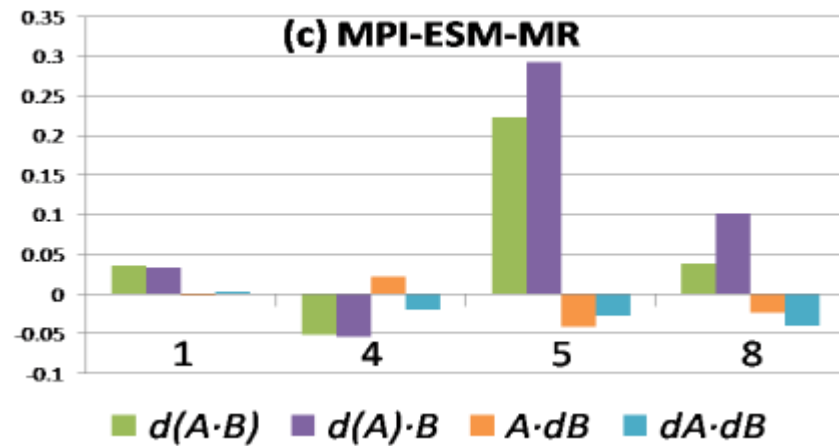
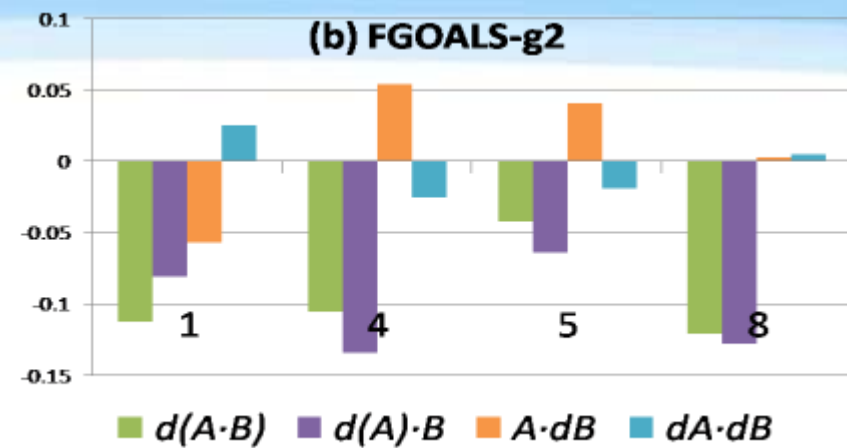
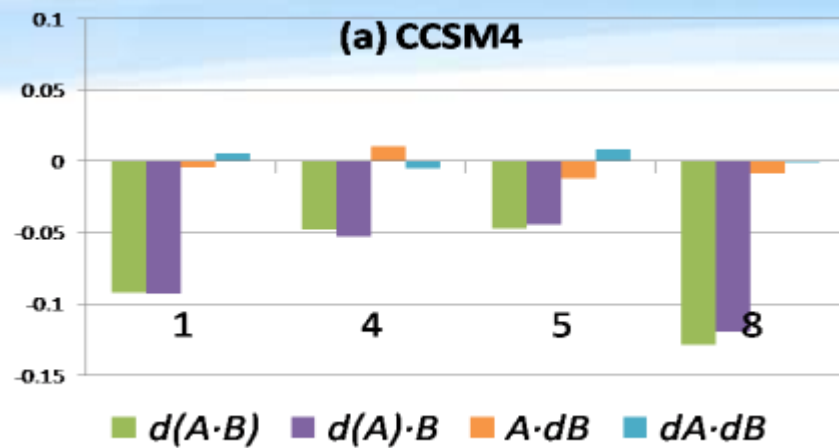
$$\partial T'/\partial t = -u' \partial \bar{T}/\partial x - \bar{u} \partial T'/\partial x - u' \partial T'/\partial x - w' \partial \bar{T}/\partial z - \bar{w} \partial T'/\partial z - w' \partial T'/\partial z$$

$$(1) \quad (2) \quad (3) \quad (4) \quad (5) \quad (6)$$

$$-v' \partial \bar{T}/\partial y - \bar{v} \partial T'/\partial y - v' \partial T'/\partial y + \frac{Q'}{\rho C_p H} + R$$

$$(7) \quad (8) \quad (9) \quad (10)$$

Relative Role of Perturbation vs. Mean State Changes



→ The **change of perturbation** is critical for the diverged ENSO amplitude projections. This indicates that the **direct** impact of the mean state change is negligible.

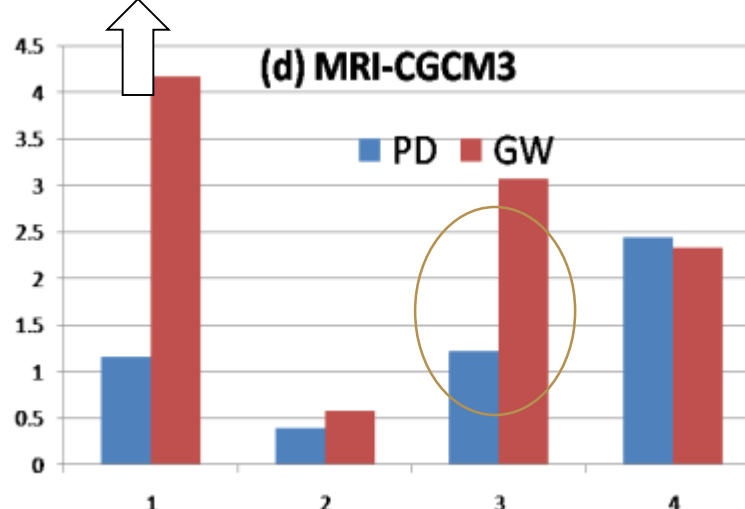
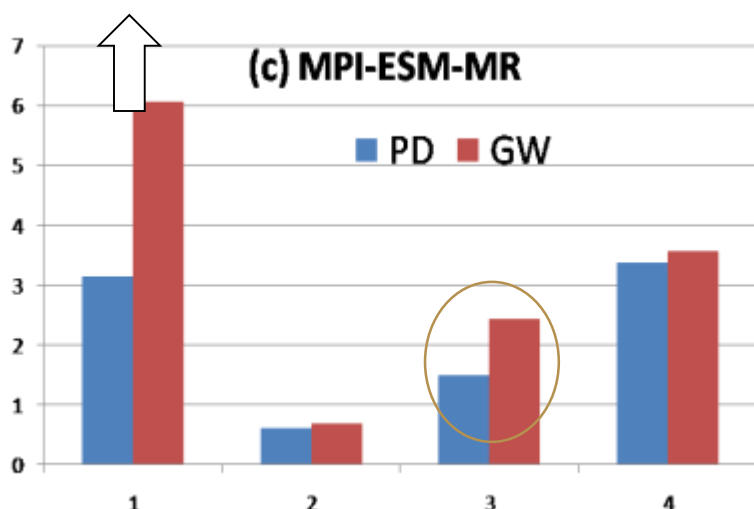
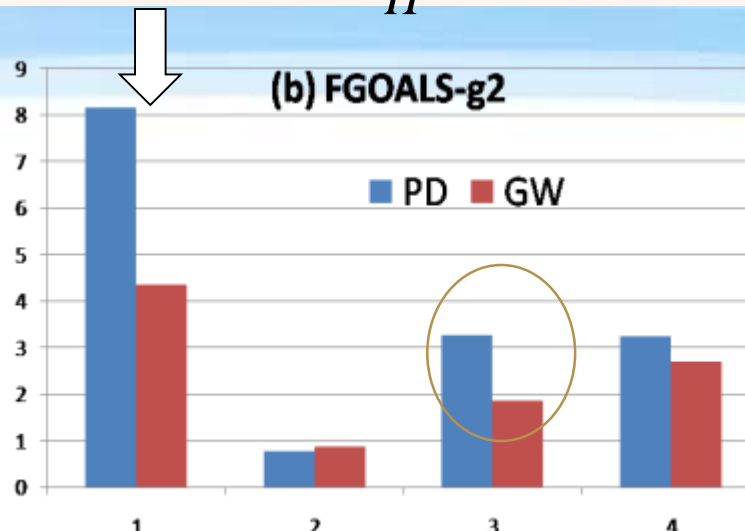
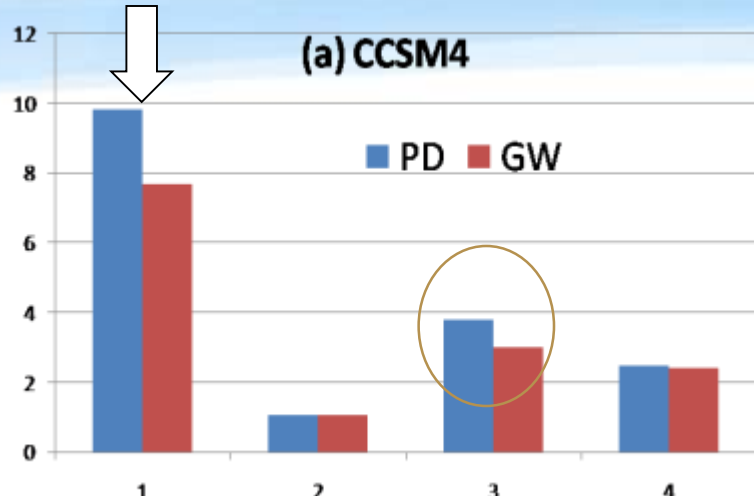
Bjerknes TH Feedback (Liu, Li et al. 2012, J. Climate):

Growth rate: $\sigma = \frac{\bar{w}}{H} R(\tau_x', T') R(D', \tau_x') R(T_e', D')$

Science Question 3:

The Bjerknes TH feedback involves 1) **how the atmospheric wind responds to unit SSTA forcing**, 2) **how strong the ocean TH responds to unit wind stress forcing**, and 3) **how strong the subsurface temperature responds to unit TH change**. **Which feedback coefficient change is critical in determining the ENSO amplitude change?**

Bjerknes TH Feedback (Liu et al. 2012): Growth rate $\sigma = \frac{\bar{w}}{H} R(\tau_x', T') R(D', \tau_x') R(T_e', D')$

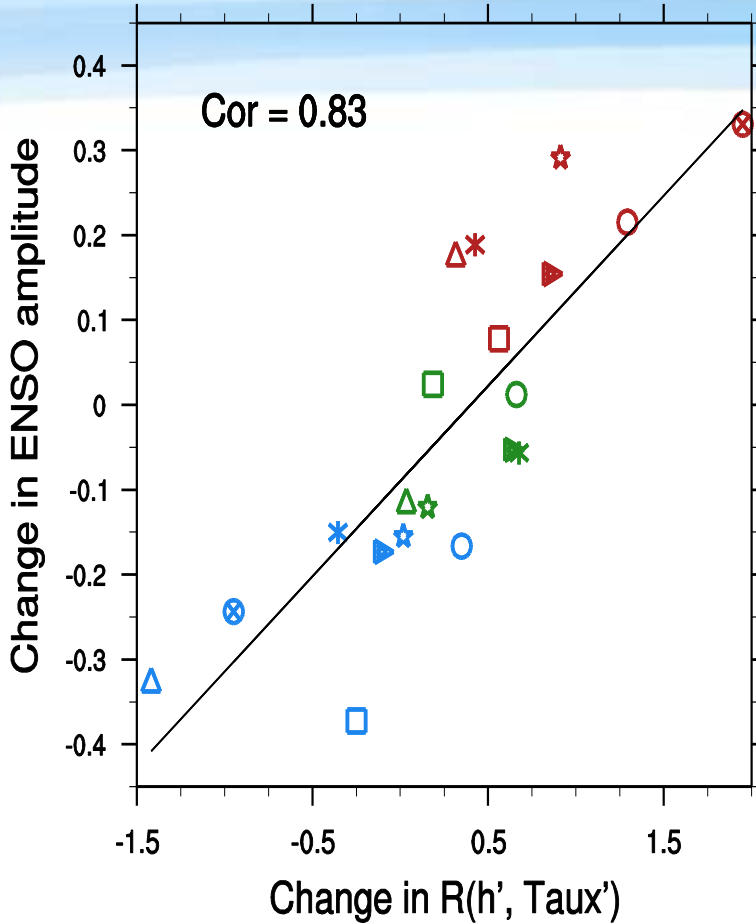


bar 1: $R(\tau_x', T') R(D', \tau_x') R(T_e', D')$.

Page ■ 31

bar2: $R(\tau_x', T')$; bar3: $R(D', \tau_x')$; bar4: $R(T_e', D')$.

ENSO Amplitude Change vs. R (h', Taux') in 20 CMIP5 models



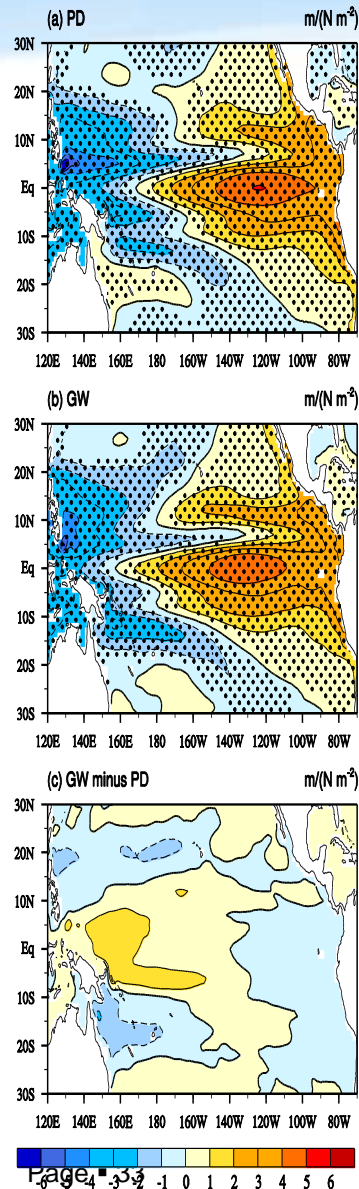
ST: 7 ENSO strengthened model group (red);

WK: 7 ENSO weakened model group (blue).

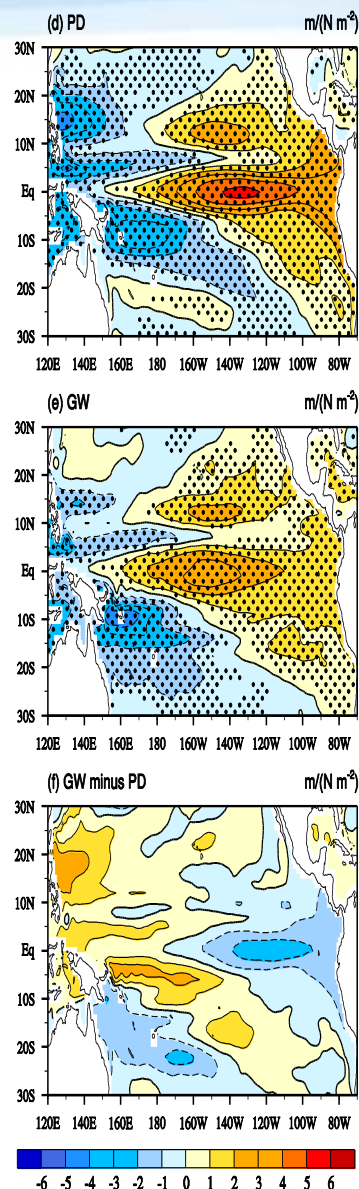
A further analysis shows that in **ZA feedback**, u' is primarily determined by **geostrophic current anomaly**, which is also related to **the TH anomaly**. Thus, **the distinctive changes of thermocline response to the wind forcing** hold a key for explaining the ENSO amplitude change under GW.

Thermocline-depth patterns regressed onto Nino4 Taux anomaly

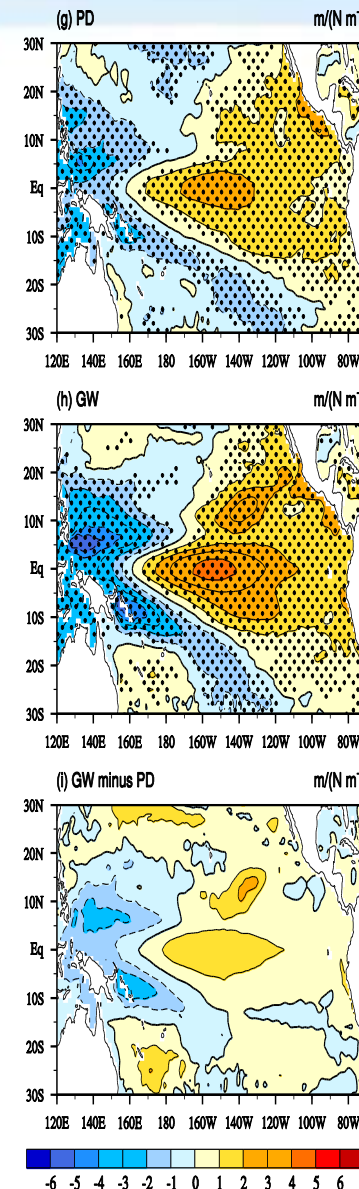
CCSM4



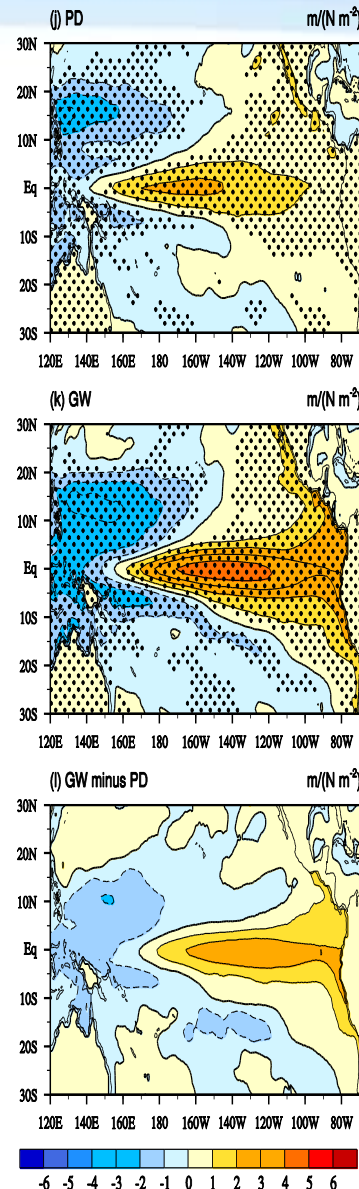
FGOALS-g2



MPI-ESM-MR



MRI-CGCM3



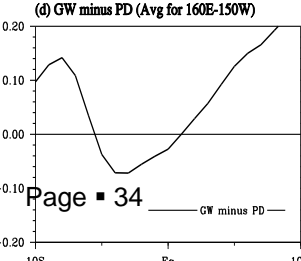
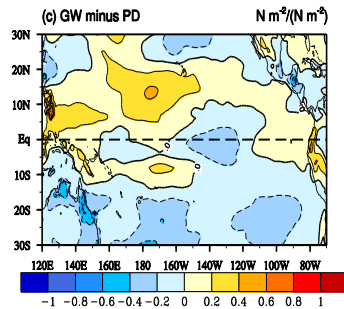
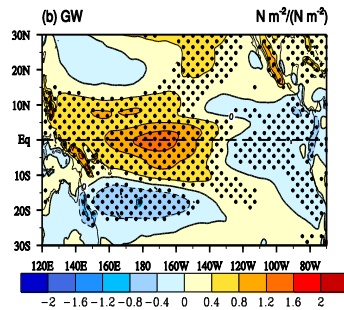
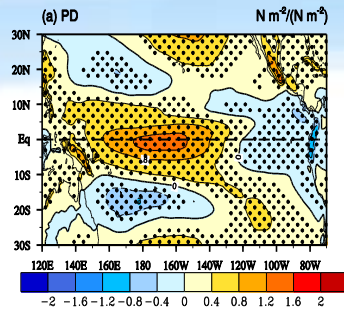
PD

GW

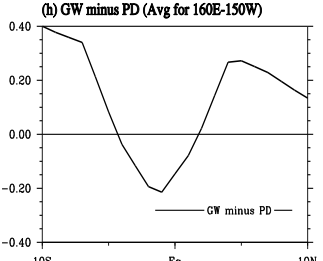
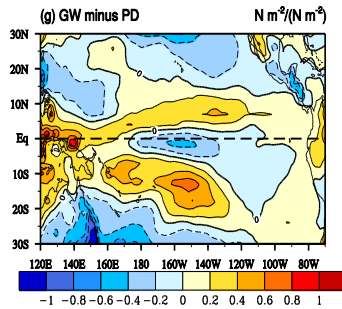
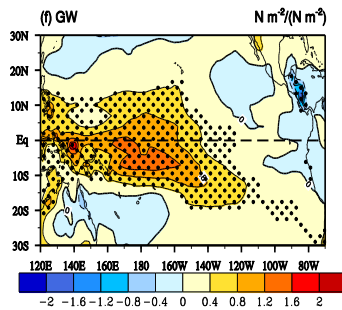
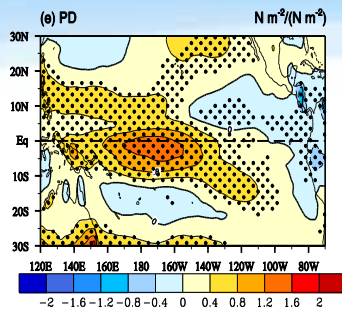
GW — PD

What causes distinctive TH responses? → Change of meridional profile of Taux'

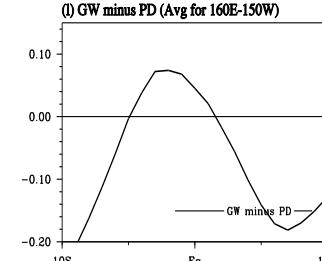
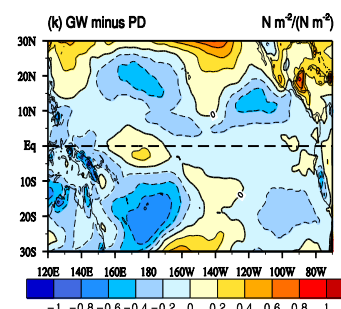
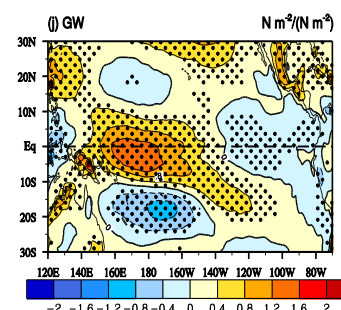
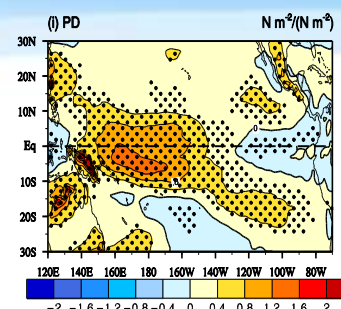
CCSM4



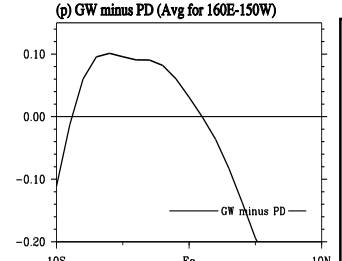
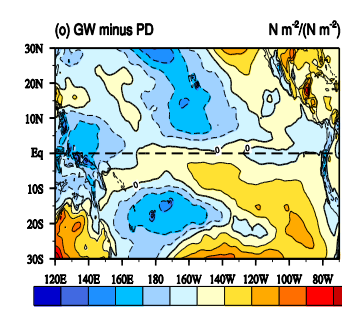
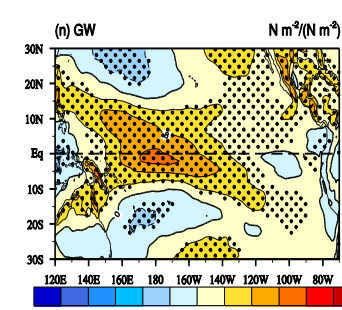
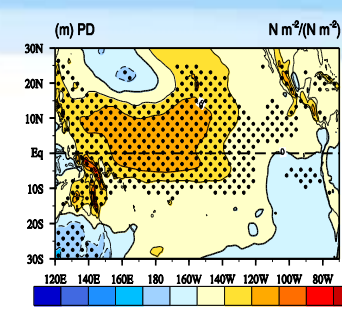
FGOALS-g2



MPI-ESM-MR



MRI-CGCM3



PD

GW

GW—
PD

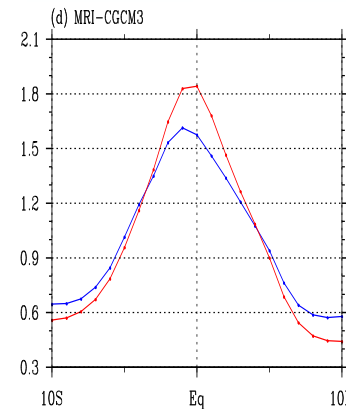
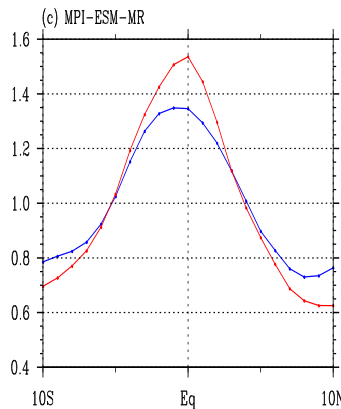
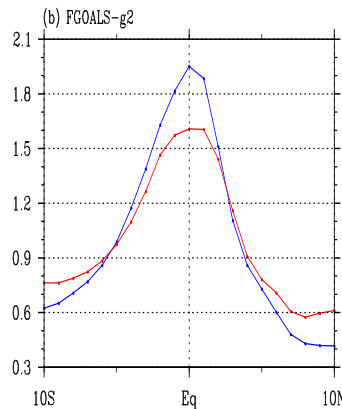
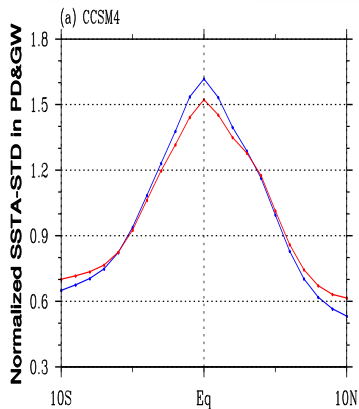
Taux'
regressed
onto Nino4
Taux' index

Change of Meridional Width of SSTA

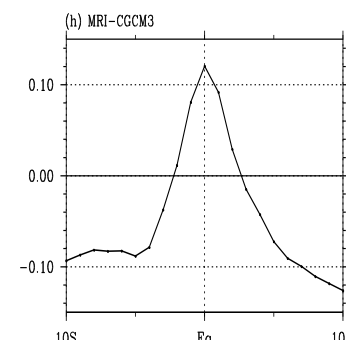
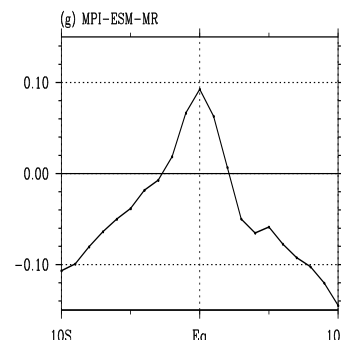
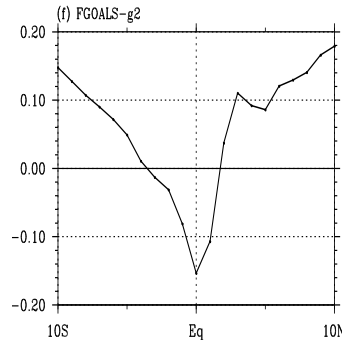
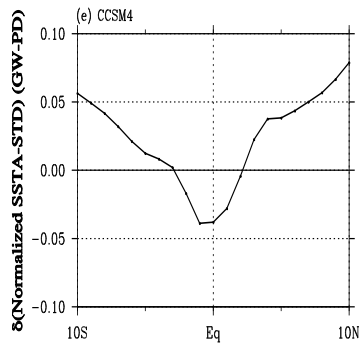
SSTA-Std regressed onto the Nino3 index

PD

GW

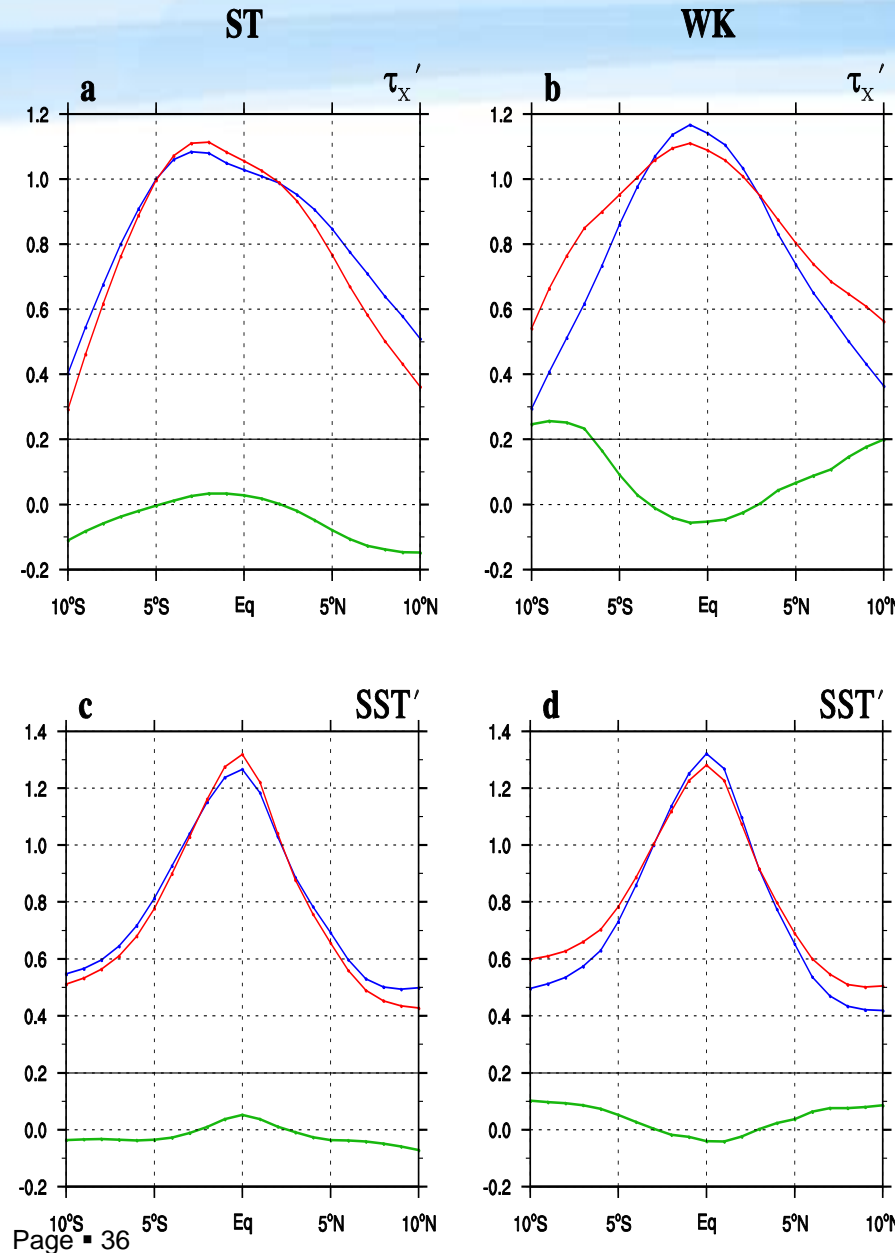


— (GW-PD)



→ Decreased (increased) meridional scale of TauxA and SSTA was found in the CGCMs with strengthened (weakened) ENSO amplitude.

Meridional Structure Change of Taux' and SSTA in 20 CMIP5 Models



(Top) Regressed Taux' averaged over 160°E-150°W for ST and WK groups

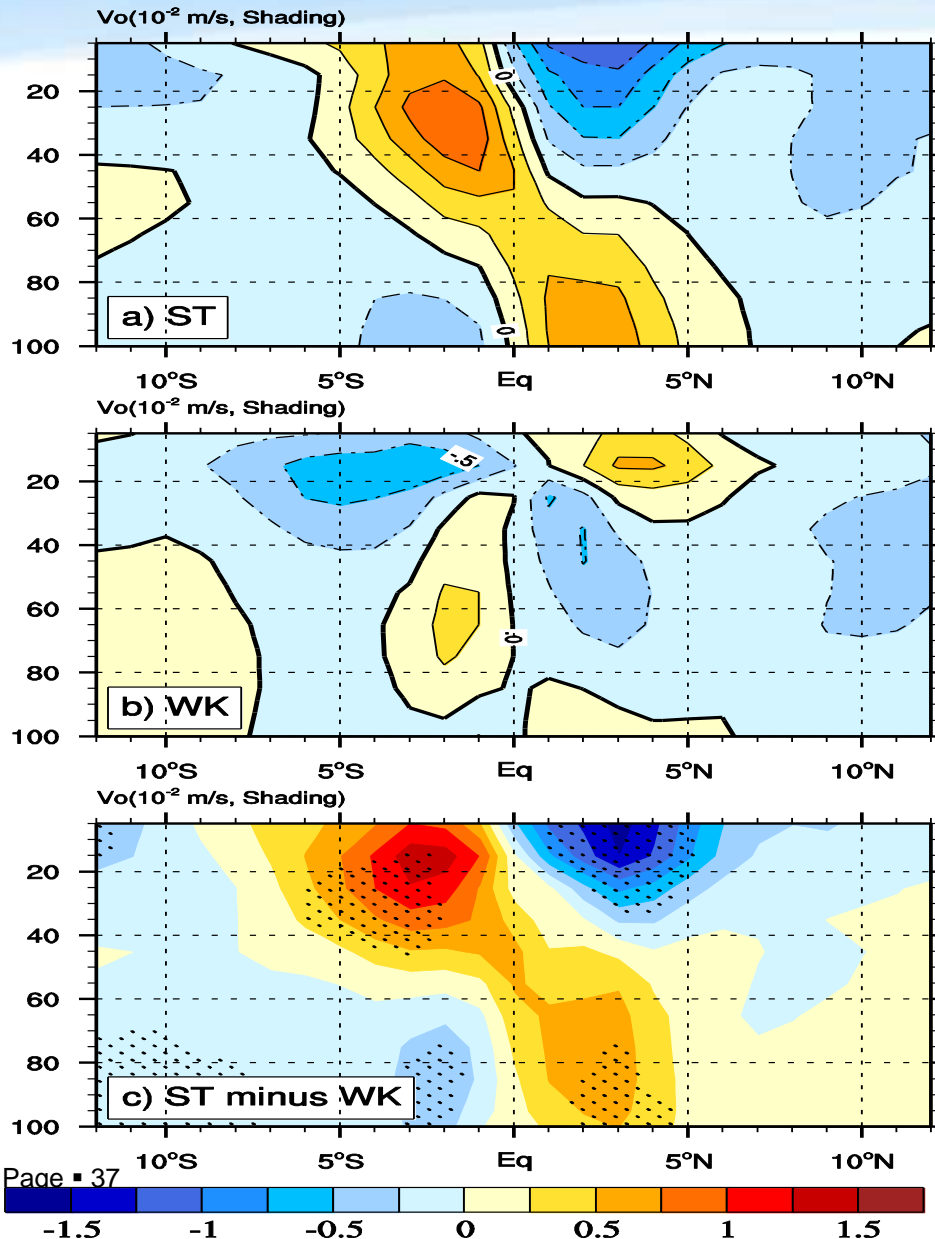
(Bottom) Regressed SSTA averaged over 150°W-90°W.

Blue: PD; Red: GW; Green: GW-PD

→ In the ST (WK) group, Taux' and SSTA patterns become more sharp (flat) in their meridional structures under GW.

Changes of the Mean STC Intensity (ST vs. WK Group)

Meridional Ocean Current Change



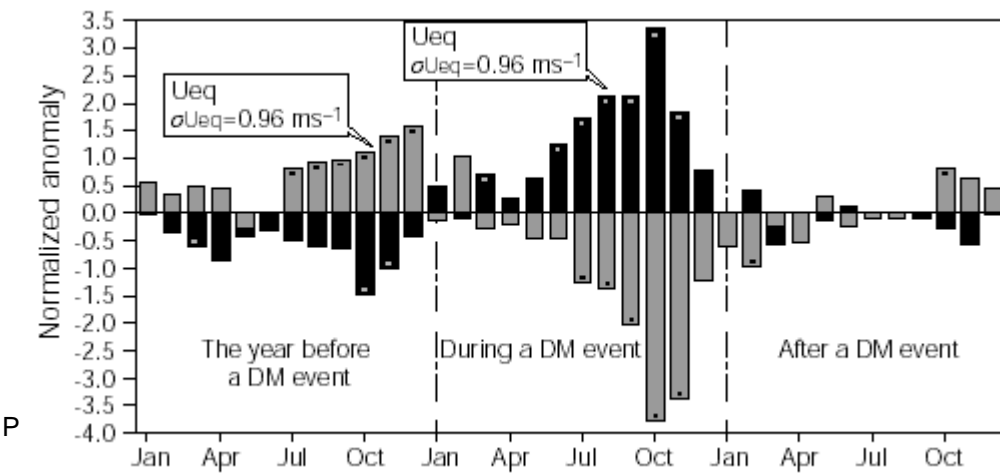
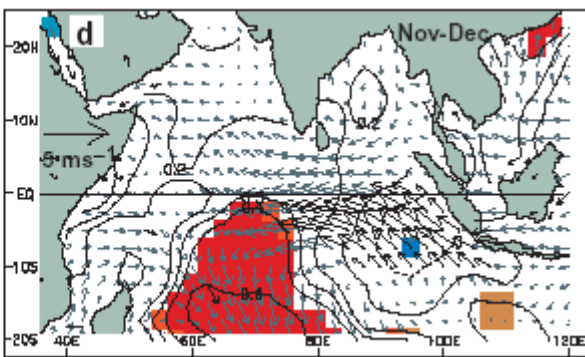
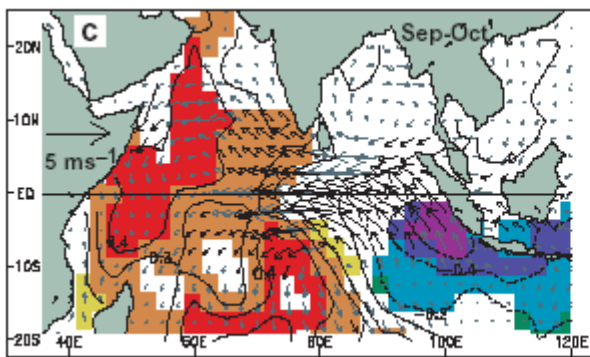
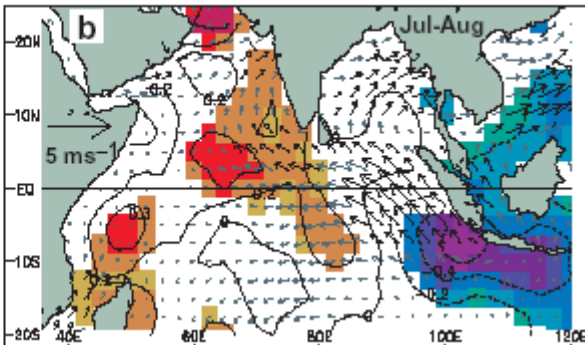
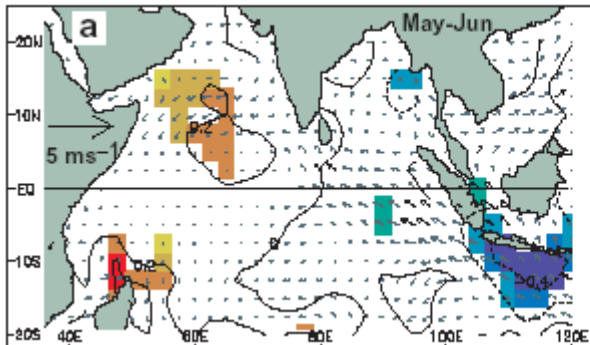
(Left) Composite meridional ocean current change averaged over 160E-90W for **ST** (top) and **WK** (middle) groups and **their difference** (bottom, **ST minus WK**)

The **stippling** in the bottom panel indicates that the difference exceeds a **95% confidence level** using Student's t-test.

Conclusion

- ENSO amplitude changes in 20 CMIP5 models are primarily controlled by Bjerknes TH and ZA feedback changes, both of which are determined by distinctive changes of TH response to unit wind stress forcing.
- The change of the mean state does not directly affect ENSO amplitude change but does indirectly affect it through the change of mean Subtropical Cell, which affects the meridional width of ENSO and thus coupled air-sea feedback strength.

Example 3: Diagnosis of the Indian Ocean Dipole



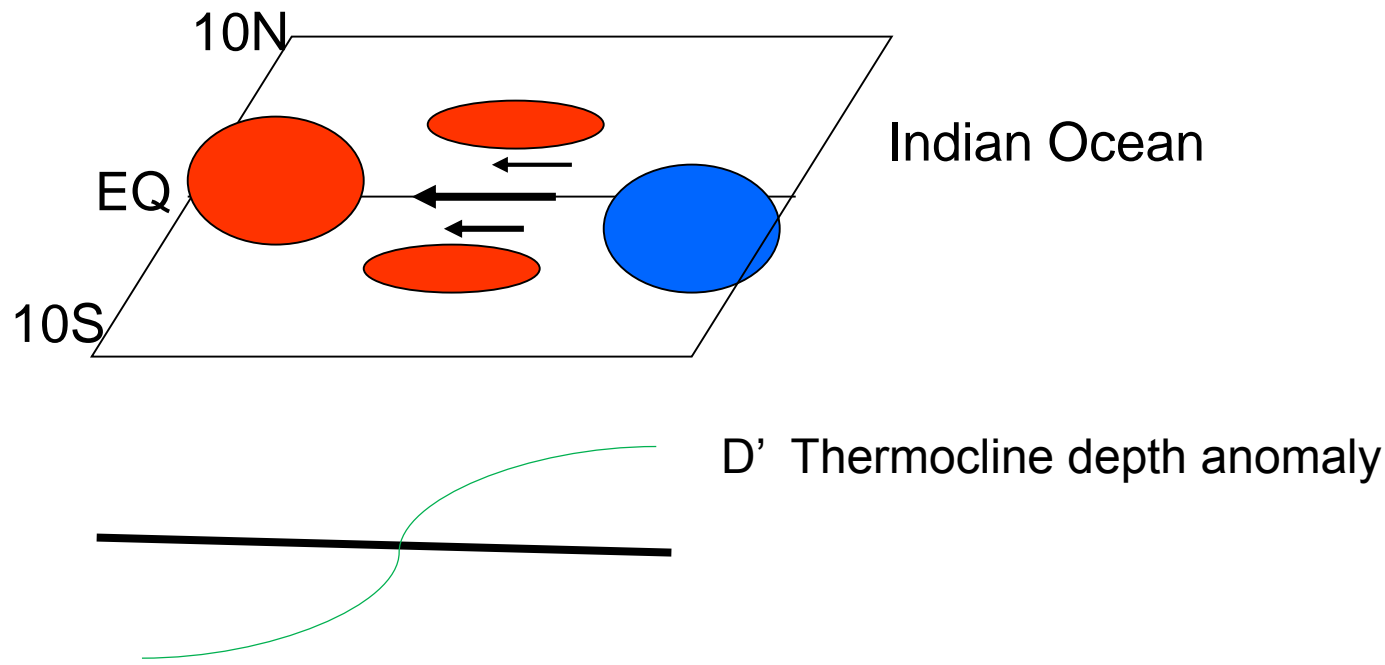
El Nino-like Variability in the Indian Ocean → Indian Ocean dipole (IOD)

- 1) IOD is an air-sea coupled mode in Indian Ocean.
- 2) It involves Bjerknes' dynamic feedback.
- 3) Its peak phase occurs in northern fall, different from El Nino which is mature in northern winter.
- 4) IOD has a great impact on Asian monsoon and East Asia climate.

(POSITIVE IOD PHASE :
1961, 1967, 1972, 1982, 1994, 1997)

Saji et al. 1999

Schematic of Bjerknes dynamical feedback during IOD development

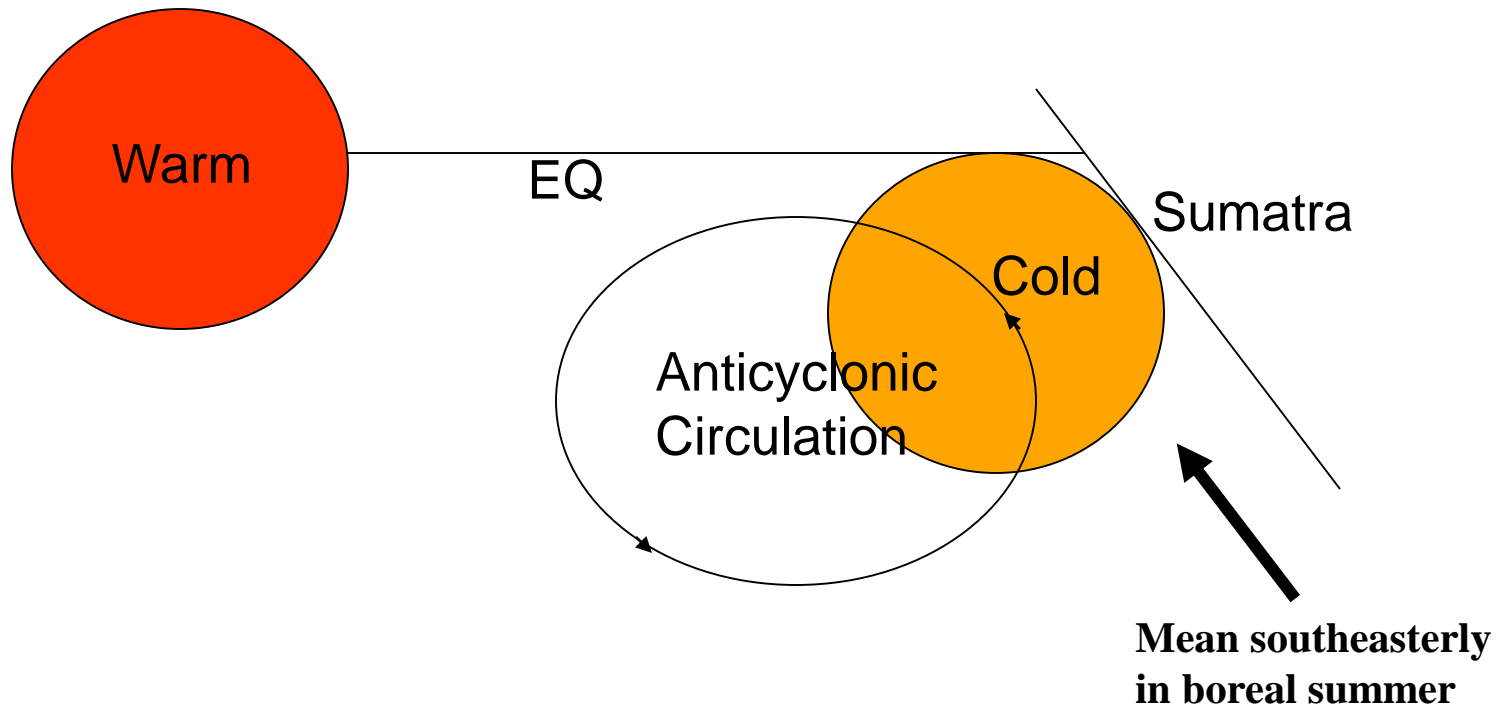


Steps to diagnose the Bjerknes dynamic feedback in a coupled model:

- 1.R(u' , T')
- 2.R(D' , u')
- 3.R(T_e' , D')

A Season-dependent Thermodynamic Air-Sea Feedback in the Southeast Indian Ocean

(Li et al. 2003, J. Atmos. Sci.)

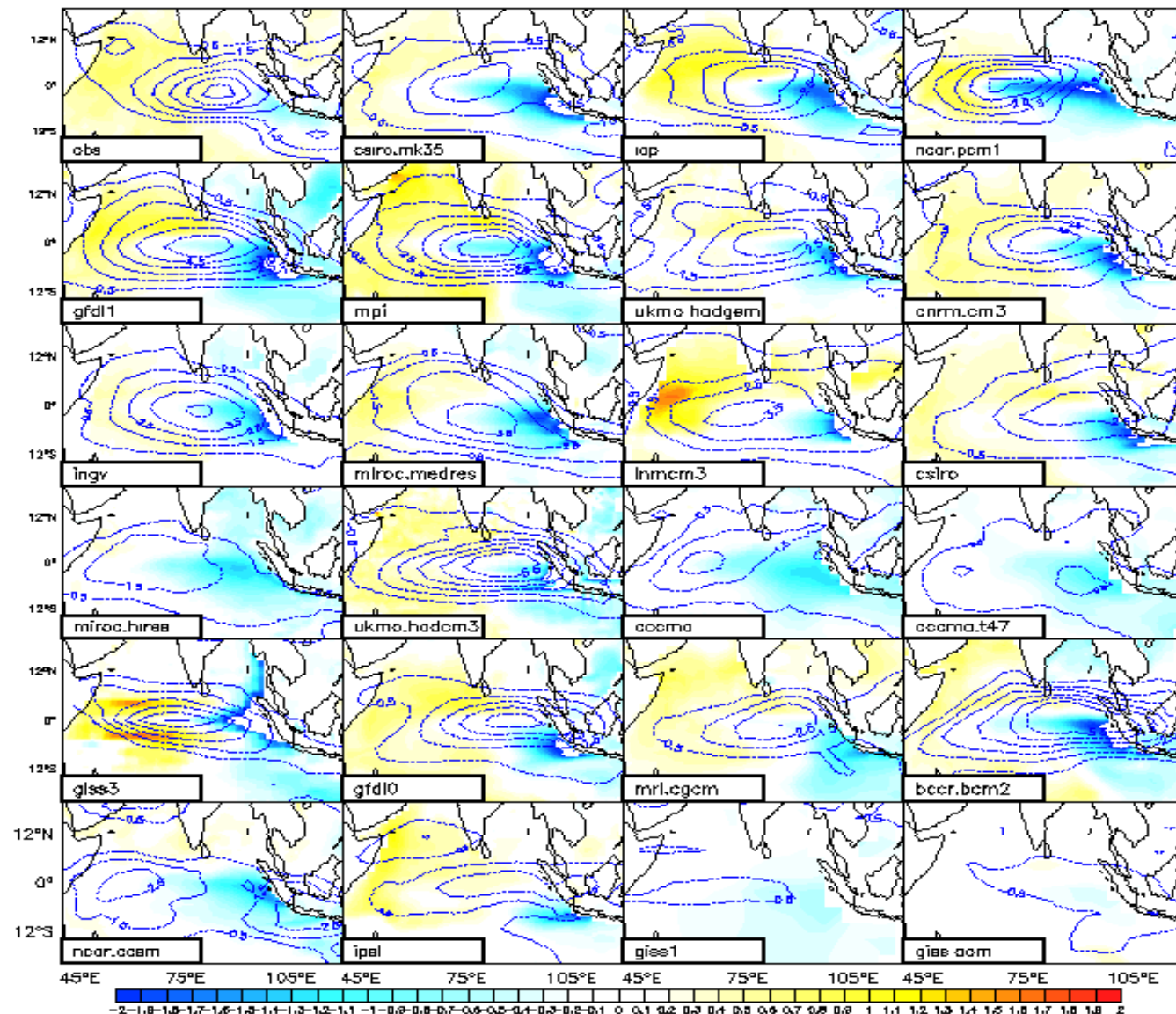


Boreal summer: **Positive** feedback

Boreal winter: **Negative** feedback

This explains why IOD peaks in boreal fall.

Composite SSTA (shading) and 850-hPa zonal wind anomaly fields in SON from the observation and 23 AR4 models



Rank the IOD simulation strength

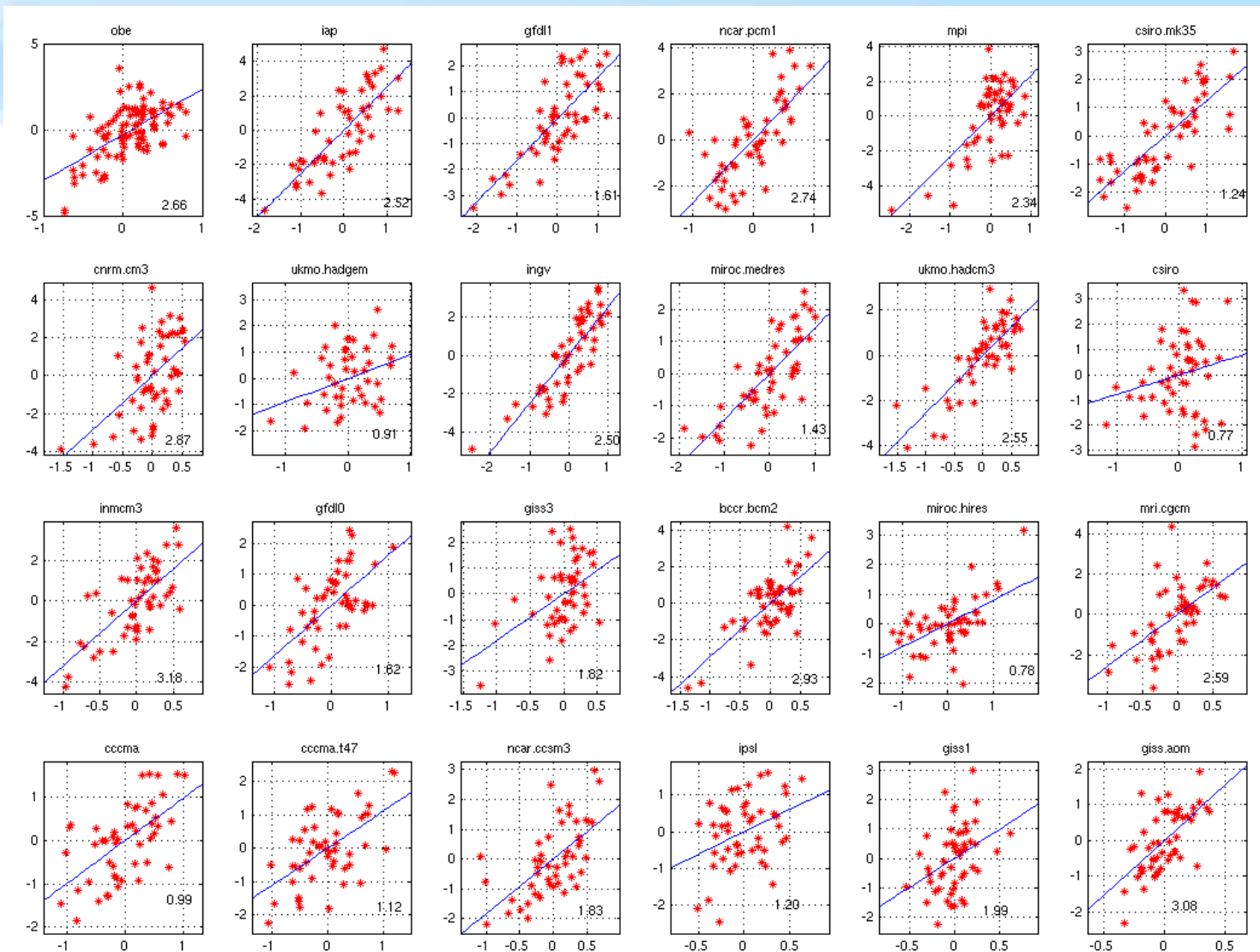
No.	ISI	DMI	EDMI	Model short name	CMIP model names
1	4.608	1.369	0.863	iap	FGOALS-g1.0
2	4.015	1.145	0.853	gfdl1	GFDL-CM2.1
3	3.841	1.242	0.874	ncar.pcm1	PCM
4	3.723	1.052	0.758	mpi	ECHAM5/MPI-OM
5	3.445	1.287	1.029	csiro.mk35	CSIRO-Mk3.5
6	2.904	1.014	0.707	cnrm.cm3	CNRM-CM3
7	2.687	0.787	0.644	ukmo.hadgem	UKMO-HadGEM1
8	2.455	0.886	0.722	ingv	INGV-SXG
9	2.417	0.920	0.687	miroc.medres	MIROC3.2(medres)
10	2.414	0.719	0.501	ukmo.hadcm3	UKMO-HadCM3
11	2.302	0.797	0.595	csiro	CSIRO-Mk3.0
12	2.203	0.963	0.525	inmcm3	INM-CM3.0
13	1.606	0.627	0.464	gfdl0	GFDL-CM2.0
14	1.393	0.631	0.481	giss3	GISS-EH
15	1.359	0.498	0.429	bccr.bcm2	BCCR-BCM2.0
16	1.323	0.638	0.609	miroc.hires	MIROC3.2(hires)
17	1.171	0.628	0.443	mri.cgcm	MRI-CGCM2.3.2
18	1.103	0.549	0.615	cccma	CGCM3.1(T63)
19	0.956	0.556	0.583	cccma.t47	CGCM3.1(T47)
20	0.700	0.424	0.424	ncar.ccsm3	CCSM3
21	0.661	0.401	0.315	ipsl	IPSL-CM4
22	0.330	0.240	0.272	giss1	GISS-ER
23	0.158	0.201	0.207	giss.aom	GISS-AOM

S

M

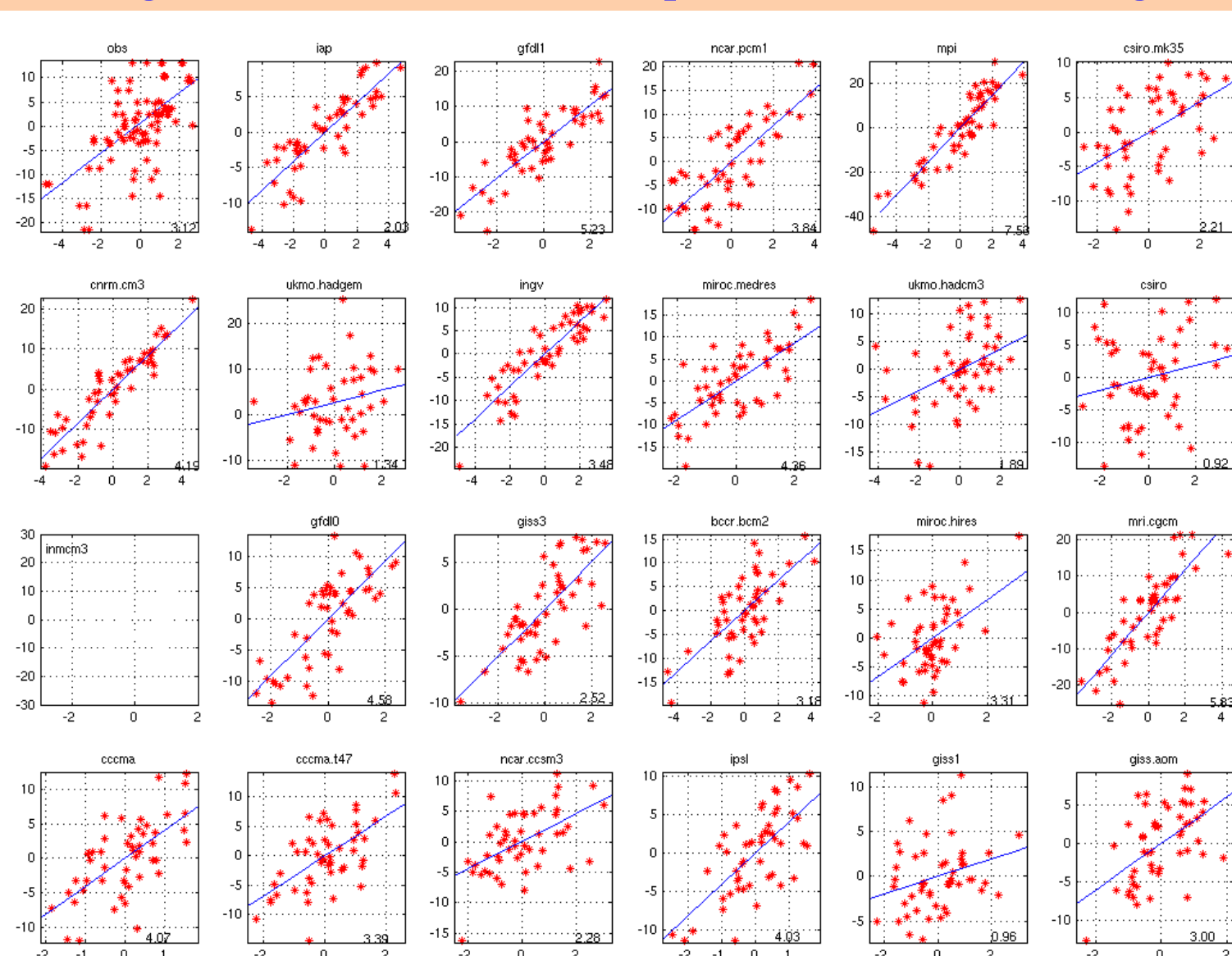
W

Diagnose the strength of atmospheric response to unit SSTA forcing, $R(u', T')$



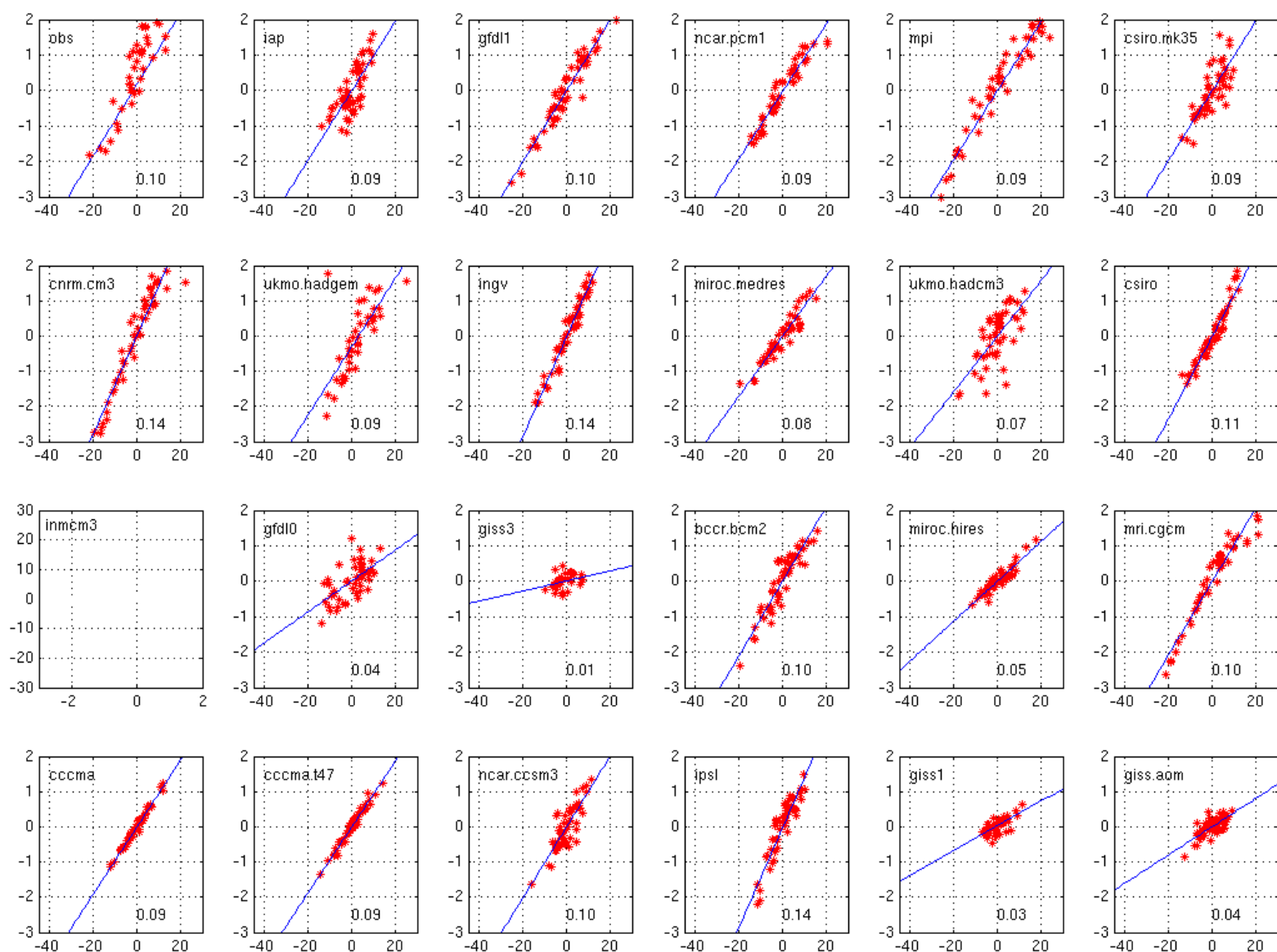
Scatter diagram between 850-hPa zonal wind anomaly in CEIO and SSTA in SEIO during the IOD developing phase (JAS) for the observation (top left) and each of the 23 AR4 models

Diagnose strength of ocean thermocline response to unit wind forcing, $R(D', u')$



Scatter diagram between thermocline depth anomaly in SEIO
and 850-hPa zonal wind anomaly in CEIO

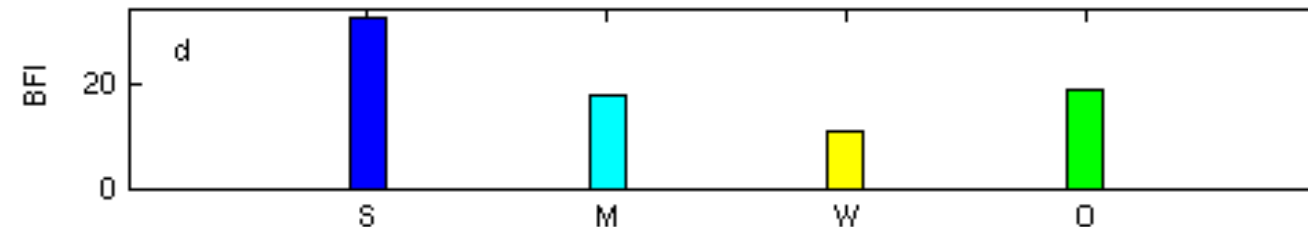
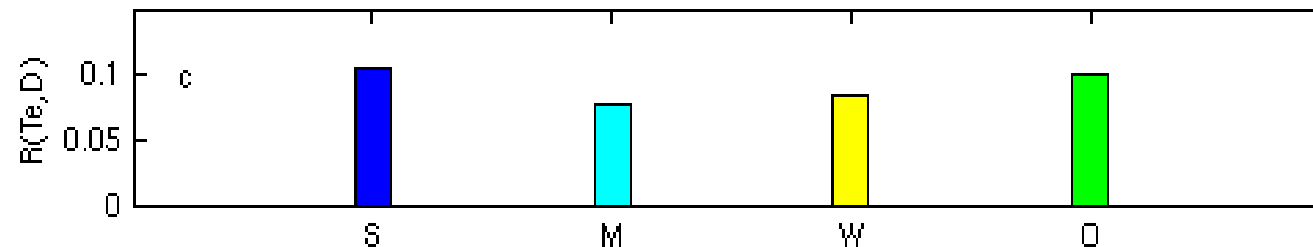
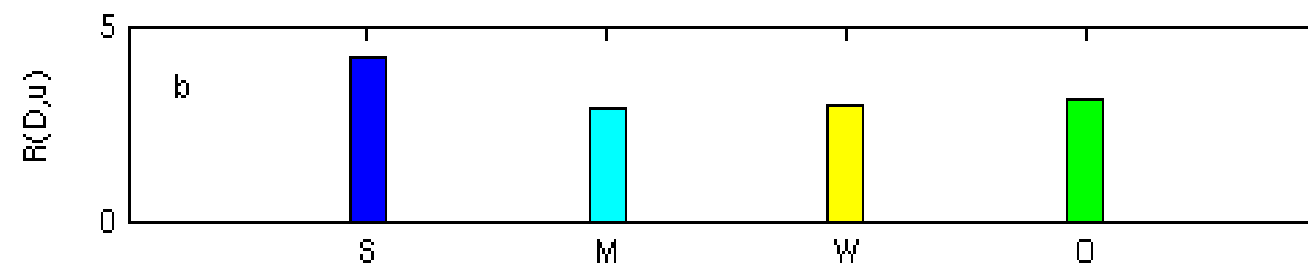
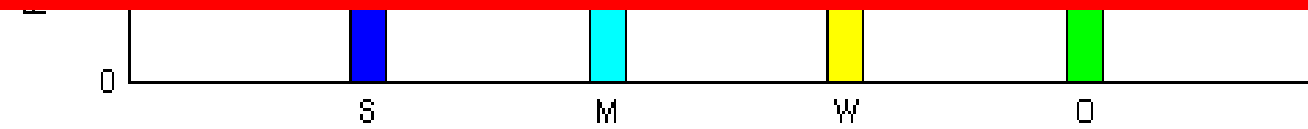
Diagnose response of subsurface temp. to unit thermocline change, R(Te', D')



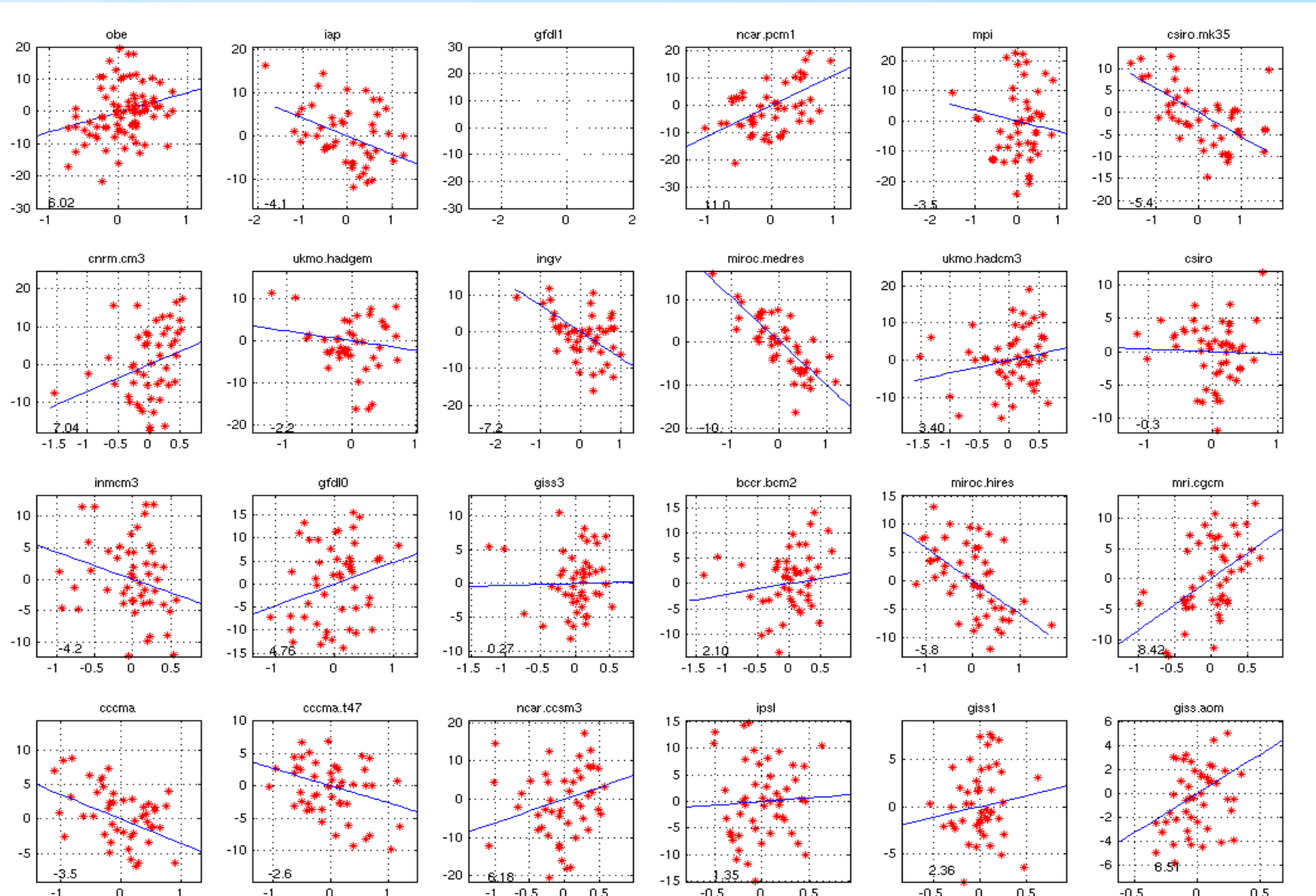
Scatter diagram between subsurface temperature anomaly and thermocline depth anomaly in SEIO

$R(u,T)$, $R(D,u)$, $R(Te,D)$ for strong, moderate and weak model groups and from the observations

REMARKS

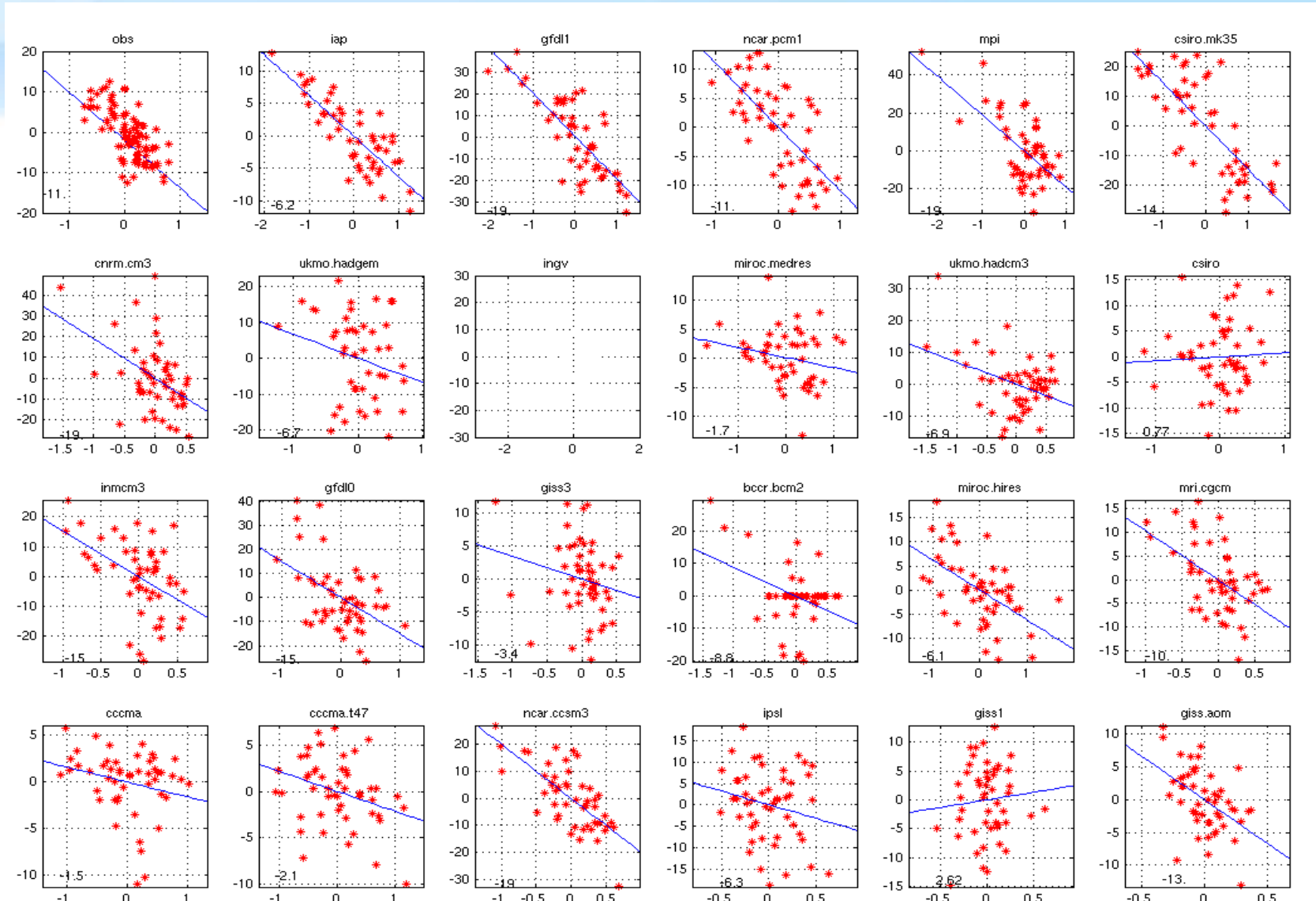


Diagnose the response of surface LHF to unit SSTA change, R(LHF', T')



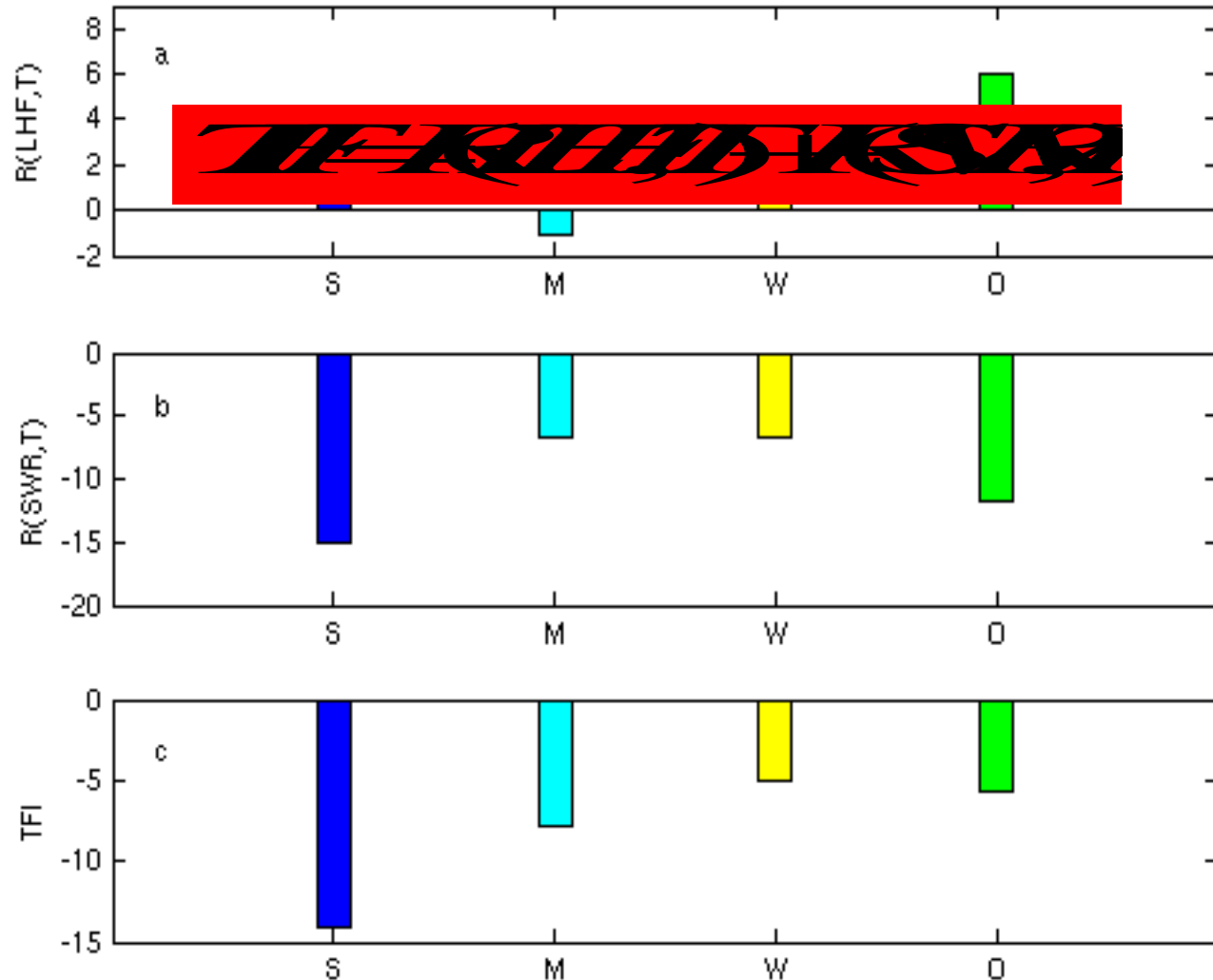
Scatter diagram between the surface latent heat flux (LHF) anomaly and SSTA in SEIO

Diagnose the response of surface SWR to unit SSTA change, $R(SWR', T')$

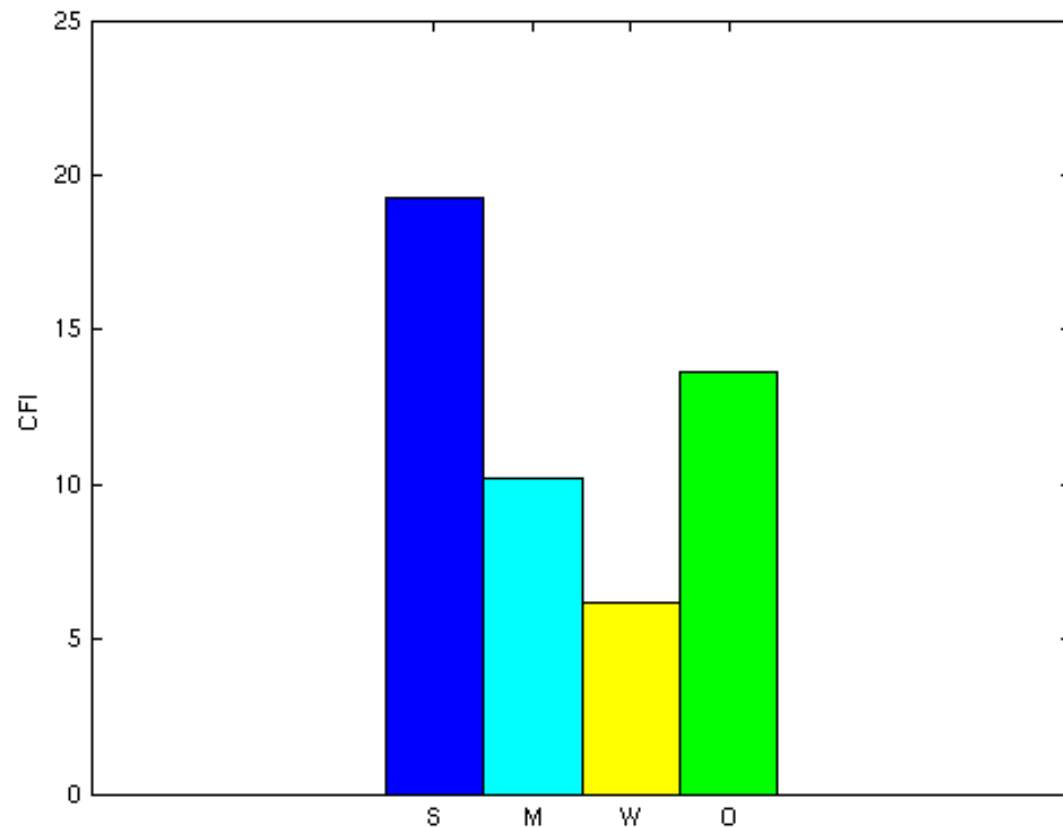


Scatter diagram between the surface net shortwave radiation anomaly and SSTA in SEIO

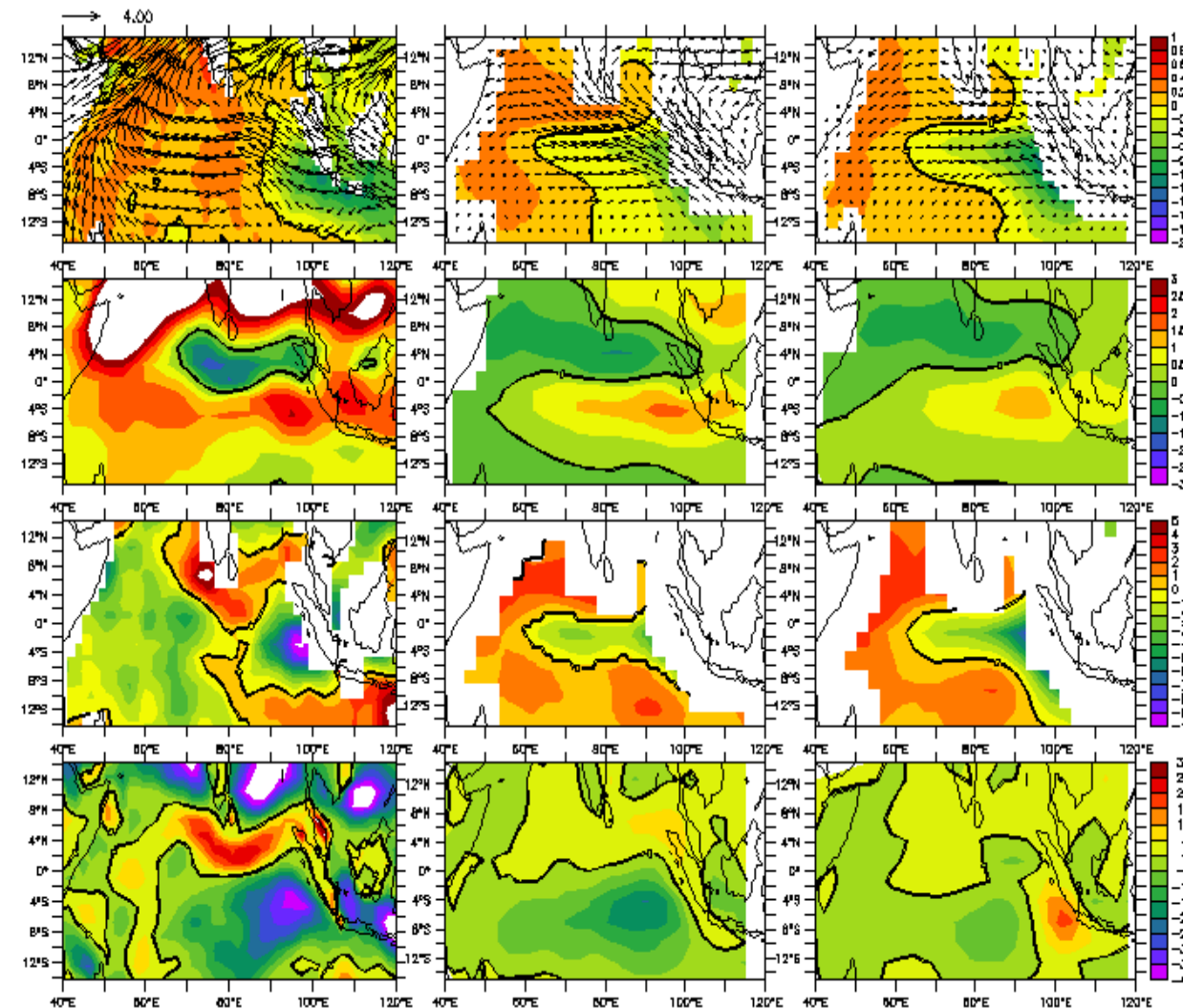
$R(LHF,T)$ and $R(SWR,T)$ for the strong, moderate and weak composites and from the observations



CFI during the IOD developing phase (JAS) for the strong, moderate and weak composites and from the observations



Why did some CGCMs generate a positive LHF-SST feedback while others generate a negative LHF-SST feedback?



Top: SST (shading) and 925-hPa wind (vector) anomalies

Second row: 925-hPa wind speed anomaly

Third row: sea-air specific humidity difference anomaly ($qs - qa$)

Bottom: surface LHF anomaly

Left: observations

Middle: positive $R(LHF, T)$ model composite

Right: negative $R(LHF, T)$ model composite during IOD developing phase

Conclusion

- The performance of 23 AR4 models in simulation of the Indian Ocean Dipole (IOD) was evaluated. A combined Bjerknes and thermodynamic feedback index was introduced. This index well reflects the simulated IOD strength and gives a quantitative measure of the relative contribution of the dynamic and thermodynamic feedback processes.
- The distinctive air-sea coupling strength among the AR4 models is partly attributed to the difference in the mean state. A shallower (deeper) mean thermocline, a stronger (weaker) background vertical temperature gradient, and a greater (smaller) mean vertical upwelling velocity are found in the strong (weak) simulation group. Thus, the mean state biases greatly affect the air-sea coupling strength on the interannual timescale.
- Some models failed to reproduce the observed positive LHF-SST feedback during the IOD development phase. The cause of this bias is attributed to the overestimate (underestimate) of effect of sea-air specific humidity (wind speed).

Thanks

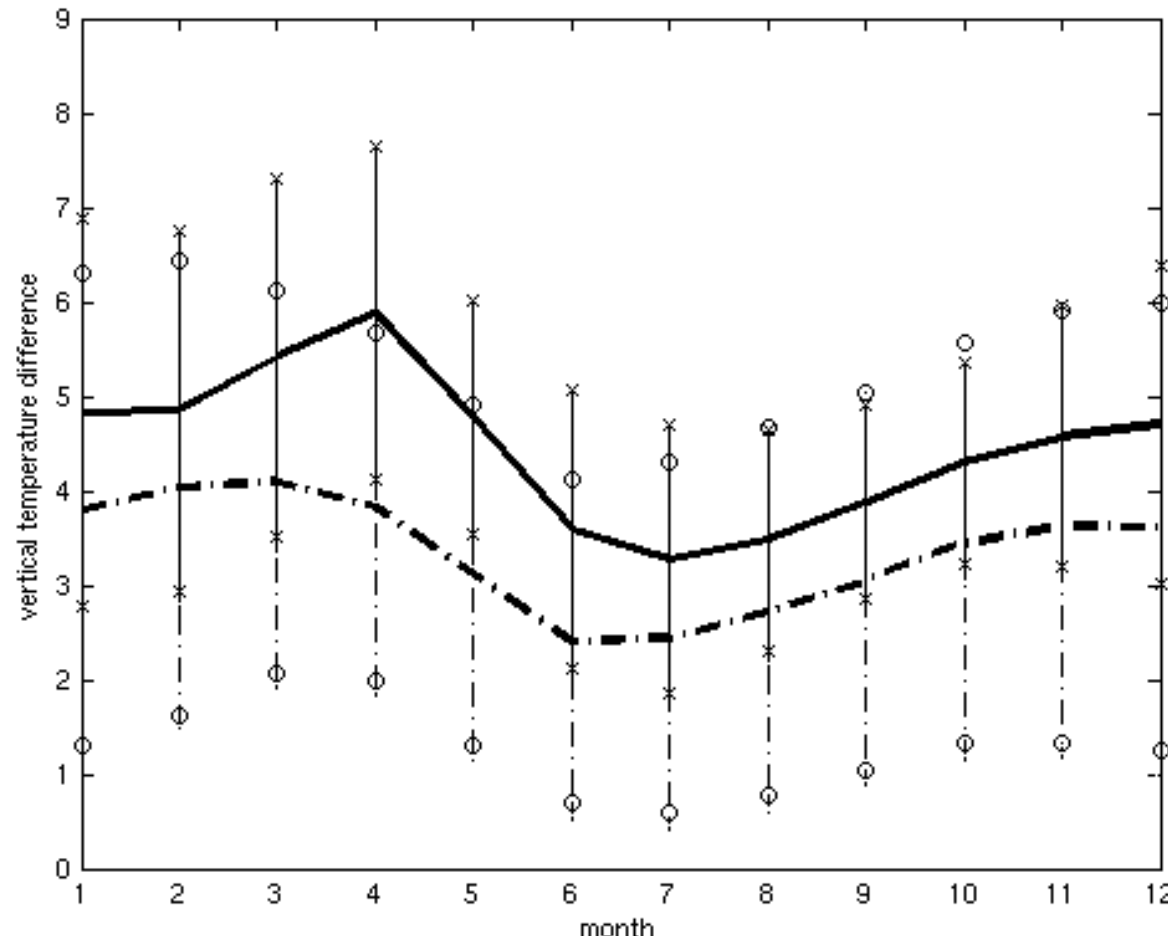
Diamond Head

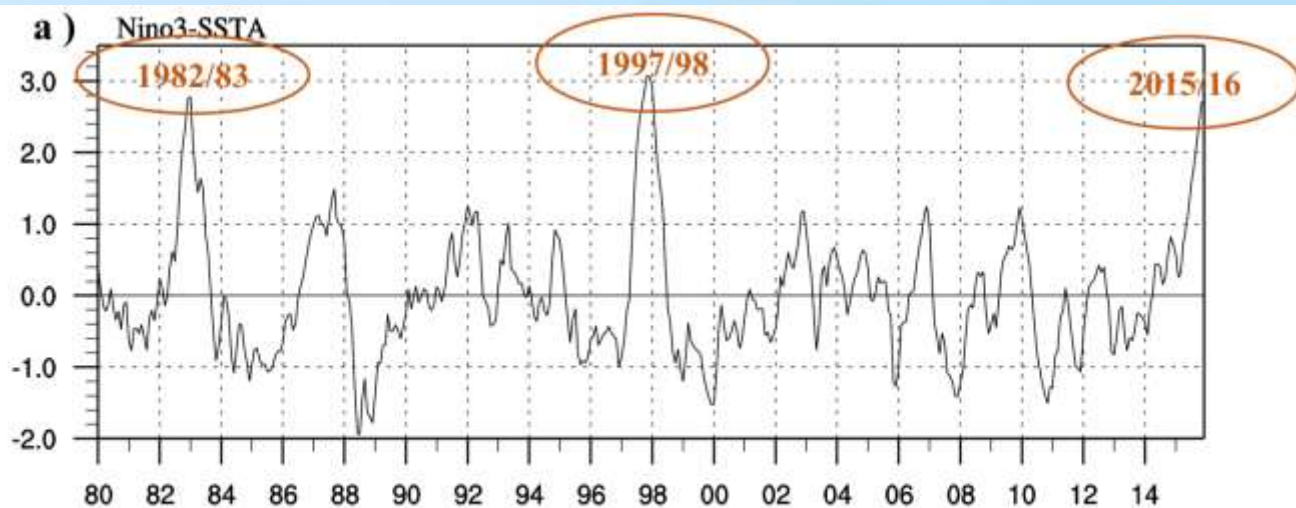


Mean state difference between strong and weak groups:

- 1) mean thermocline depth along the equator
- 2) mean w
- 3) upper-ocean vertical temperature gradient

$$w' \frac{\partial \bar{T}}{\partial z}$$





b) Time Evolution of SSTA

